

DTIC FILE COPY

4

# KINETICS OF STRUCTURAL RELAXATIONS IN A TWO-DIMENSIONAL MODEL ATOMIC GLASS - III

AD-A199 080

D. Deng <sup>1</sup>, A.S. Argon, and S. Yip  
Massachusetts Institute of Technology  
Cambridge, MA 02139

DTIC  
ELECTE  
SEP 02 1988  
S H D

Abstract



*The kinetics of structural relaxation in a two-dimensional model atomic glass quenched infinitely rapidly from the melt to 0.55 of the glass transition temperature was simulated by the molecular dynamics method to study the chronological ordering of the atomic kinematics associated with such relaxations. Over the very short periods of aging (c.a. 200 atomic fluctuations) accessible to the MD method, a Williams-Watts form of relaxation with a fractional exponent of 0.5 was found to hold for excess enthalpy, free volume, and site distortion parameter. The distribution of free energy barriers associated with this relaxation that resulted from the analysis could be scaled up to describe processes occurring on macroscopic time scales, and agrees well with experimental results in  $Cu_2Zr_{1-z}$  glasses. Results on the clustering of relaxations and other topological features of the relaxation process are also reported.*

<sup>1</sup>On leave from the Institute for Precious Metals in Kunming, Yunnan Province, China

DISTRIBUTION STATEMENT A

Approved for public release;  
Distribution Unlimited

88 9 2 07 9

## REPORT DOCUMENTATION PAGE

|  |  |   |                            |
|--|--|---|----------------------------|
| 1a. REPORT SECURITY CLASSIFICATION<br>UNCLASSIFIED   |  | 1b. RESTRICTIVE MARKINGS<br>NONE  |                            |
| 2a. SECURITY CLASSIFICATION AUTHORITY  |  | 3. DISTRIBUTION AVAILABILITY OF REPORT<br>Approved for public release.<br>Distribution unlimited. |                            |
| 2b. DECLASSIFICATION/DOWNGRADING SCHEDULE  |  |   |                            |
| 4. PERFORMING ORGANIZATION REPORT NUMBER(S)<br>Technical Report No. 5  |  | 5. MONITORING ORGANIZATION REPORT NUMBER(S)   |                            |
| 6a. NAME OF PERFORMING ORGANIZATION<br>Massachusetts Institute of<br>Technology  | 6b. OFFICE SYMBOL<br>(if applicable)         | 7a. NAME OF MONITORING ORGANIZATION<br>ONR  |                            |
| 6c. ADDRESS (City, State, and ZIP Code)<br>77 Massachusetts Avenue<br>Cambridge, MA 02139  |  | 7b. ADDRESS (City, State, and ZIP Code)<br>800 North Quincy Street<br>Arlington, VA 22217         |                            |
| 8a. NAME OF FUNDING / SPONSORING<br>ORGANIZATION<br>DARPA  | 8b. OFFICE SYMBOL<br>(if applicable)         | 9. PROCUREMENT INSTRUMENT IDENTIFICATION NUMBER<br>N00014-86-K-0763                               |                            |
| 8c. ADDRESS (City, State, and ZIP Code)<br>1400 Wilson Boulevard<br>Arlington, VA 22209  |  | 10. SOURCE OF FUNDING NUMBERS   |                            |
|  |  | PROGRAM<br>ELEMENT NO.<br>R & T Code  | PROJECT<br>NO.<br>A400005  |
|  |  | TASK<br>NO.   | WORK UNIT<br>ACCESSION NO. |
| 11. TITLE (Include Security Classification)<br>KINETICS OF STRUCTURAL RELAXATIONS IN A TWO-DIMENSIONAL MODEL ATOMIC GLASS - III  |  |   |                            |
| 12. PERSONAL AUTHOR(S)<br>Deng, Derguo, Argon, Ali S., Yip, Sidney   |  |   |                            |
| 13a. TYPE OF REPORT<br>Journal paper   | 13b. TIME COVERED<br>FROM 1/15/87 TO 8/15/88 | 14. DATE OF REPORT (Year, Month, Day)<br>1988 August 22   | 15. PAGE COUNT<br>70       |
| 16. SUPPLEMENTARY NOTATION<br>Submitted to Acta Metallurgica.  |  |   |                            |
| 17. COSATI CODES   |  | 18. SUBJECT TERMS (Continue on reverse if necessary and identify by block number)                 |                            |
| FIELD  | GROUP  | SUB-GROUP   |                            |
|  |  |   |                            |
|  |  |   |                            |
| 19. ABSTRACT (Continue on reverse if necessary and identify by block number)<br><p>The kinetics of structural relaxation in a two-dimensional model atomic glass quenched infinitely rapidly from the melt to 0.55 of the glass transition temperature was simulated by the molecular dynamics method to study the chronological ordering of the atomic kinetics associated with such relaxations. Over the very short periods of aging (c.a. 200 atomic fluctuations) accessible to the MD method, a Williams-Watts form of relaxation with a fractional exponent of 0.5 was found to hold for excess enthalpy, free volume, and site distortion parameter. The distribution of free energy barriers associated with this relaxation that resulted from the analysis could be scaled up to describe processes occurring on macroscopic time scales, and agree well with experimental results in <math>\text{Cu}_x\text{Zr}_{1-x}</math> glasses. Results on the clustering of relaxations and other topological features of the relaxation process are also reported.</p> |  |   |                            |
| 20. DISTRIBUTION AVAILABILITY OF ABSTRACT<br><input checked="" type="checkbox"/> UNCLASSIFIED/UNLIMITED <input type="checkbox"/> SAME AS RPT <input type="checkbox"/> DTIC USERS   |  | 21. ABSTRACT SECURITY CLASSIFICATION<br>UNCLASSIFIED  |                            |
| 22a. NAME OF RESPONSIBLE INDIVIDUAL<br>A.S. Argon  |  | 22b. TELEPHONE (Include Area Code)<br>(617) 253-2217  | 22c. OFFICE SYMBOL         |

## I. INTRODUCTION

The atomic details of structural alterations of amorphous solids during aging below their glass transition temperatures and the consequences of this on subsequent inelastic behavior has been of considerable interest. Simulation of such complex atomic processes by computer molecular dynamics (MD) has been very informative in the past. Among the many such simulations, those of Takeuchi and coworkers [1,2] on two component atomic glasses of the  $Cu_xZr_{1-x}$  type, carried out in three dimensions have resulted in considerable insight on structural relaxations. In spite of this, however, both the kinematics and the kinetics of such relaxations remain inadequately understood. We have carried out a detailed MD simulation using the same truncated  $CuZr$  pair potentials used by Kobayashi, et al [3], but in two dimensions for the specific purpose of a more thorough understanding of the atomic mechanisms of plastic flow in simple atomic amorphous media. In three related communications, we have reported results of a simulation: on the melting and glass transition process in a two-dimensional idealized material [4] (referred to here as (I)); on the topological features of structural relaxations in such a medium, both in subcooled melts and in solids below their  $T_g$  [5] (referred to here as II); and on the details of large strain plastic shear [6] (referred to here as IV). Here, in this same series of studies, we report on the kinetics of structural relaxations below  $T_g$  in the same two-component amorphous medium modeled in two dimensions. We also give additional details of some of the topological features in the material, which is more prone to undergo structural relaxation than the average.

## II. DETAILS OF THE SIMULATION

### 2.1 The Simulation Cell

The details of the MD simulation, the choice of the interatomic pair potential of interaction, its truncation, the two-dimensional simulation cell with its periodic boundary conditions, and the normalization of parameters were given in (I). Additional details on the intensive state parameters, such as atomic level stresses, moduli, enthalpy, site distortion, and local free volume were given in (II), together with many results on the topological details of structural relaxations. The results of the simulation we present here were on the same rectangular cell containing 144 atoms of two types representing Cu and Zr, placed initially randomly, and melted and quenched, as described in (I). The simulations reported here were at a temperature of  $T^* = 0.1 (= 0.4T_m^*)$  and under a constant external normalized pressure of  $p = 1.0$ . This temperature is well below the glass transition temperature of  $T_g^* = 0.18$ . The starting state of the material was one which had seen an essentially infinite quenching rate (path EF in Fig. 1 of II) from the melting temperature of 0.25, i.e., the starting material had a fictive temperature equal to the equilibrium melting temperature. Many topological details of structural relaxation of this quenched glass were reported in II. The magnitude of the so-called boundary mass used in the present simulation to maintain the external pressure constant was 4. The concept of a boundary mass associated with the volume of the simulation cell as an extra degree of freedom to maintain the external pressure constant was introduced by Andersen [7]. It has been widely used in MD simulations where only equilibrium structural prop-

erties are of interest, and the kinetics of reaching the equilibrium is not. In this simulation, however, where the kinetics of structural relaxation were of equal interest as the topological details of the atom exchanges, the proper choice of the boundary mass was an important consideration.

## 2.2 Choice of Boundary Mass in the Simulation

In the method of Andersen [7], simulation under constant external pressure is accomplished by the introduction of a new dynamic variable  $Q$  that represents the changes in the overall volume of the simulation cell. Then, the equations of motion of all  $n$  atoms in the system and the cell volume are derivable from a modified Lagrangian  $L$  given by <sup>1</sup>

$$L(\rho_i, \dot{\rho}_i, Q, \dot{Q}) = \frac{1}{2}mQ^{2/3} \sum_{i=1}^n \dot{\rho}_i \cdot \dot{\rho}_i - \frac{1}{2} \sum_{\substack{j \neq i \\ i}}^n \phi(Q^{1/3} \rho_{ij}) + \frac{1}{2}M\dot{Q}^2 - \alpha Q, \quad (1)$$

where  $\rho_i = (r_i/Q^{1/3})$  are dimensionless position coordinates of the  $n$  atoms,  $\dot{\rho}_i$ , their velocities,  $\rho_{ij}$ , the dimensionless relative separations of atoms  $i$  and  $j$ ,  $\phi$  the pair potential,  $m$  the mass of an atom,  $Q$  the coordinate representing the volume viewed as a one dimensional entity, such as the length of a cylinder capped by a piston,  $\alpha$  a constant to be interpreted as the external force resulting from the external pressure acting across the boundaries of the simulation cell in a work conjugate sense with the volume coordinate  $Q$ , and finally  $M$ , the

<sup>1</sup>All symbols not specifically defined here are the same that have been used in (I) [4], where a full list of symbols can be found.



|      |                                     |
|------|-------------------------------------|
| For  | <input type="checkbox"/>            |
| &I   | <input checked="" type="checkbox"/> |
| AS   | <input type="checkbox"/>            |
| Dist | <input type="checkbox"/>            |

|                    |         |
|--------------------|---------|
| Distribution/      |         |
| Availability Codes |         |
| Dist               | Special |
| A-1                |         |

so-called boundary mass. In Eqn. (1), the first two terms on the RHS represent the normal Lagrangian of the system of  $n$  particles if  $Q$  is interpreted as the volume. The third and fourth terms relate to the Lagrangian of the total volume of the cell in the interpretation of  $Q$  as the added dynamic variable representing the volume. The generalized velocities and momenta that result from this scaled Lagrangian, and how they can be related to the real system has been discussed in detail by Andersen [7] and need not be repeated here. It should suffice, however, to observe that the introduction into the system of a pseudo coordinate to represent the volume and a pseudo mass associated with it permits maintaining the external pressure constant by permitting the volume to change as necessary. Clearly, however, this introduces into the simulation system a new normal mode and a new momentum with an added normal mode frequency that can interact with the other physically meaningful modes of atoms, and may result in unwanted resonances. It can be shown, and is also readily clear that the introduction of this pseudo coordinate does not affect the equilibrium properties of the system and its topological features in equilibrium. It will, however, influence the kinetics of reaching equilibrium, and the topological features of non-equilibrium states that are of interest in the simulation. Andersen has proposed that unwanted artifacts in the kinetics can be reduced if the boundary mass  $M$  is chosen, so that the period of the fluctuation of  $Q$  in the scaled system is approximately equal to  $Q^{1/3}$  divided by the speed of sound in the simulation medium, when  $Q$  is equated to the volume. For a simulation cell containing 144 atoms, this rule results in a boundary mass  $M = 3.65m$  of individual atom masses. We have taken 4 as the nearest integer value to be used in the simula-

tion. In addition, however, we have tried simulations of structural relaxations with boundary masses of 400 and  $4 \times 10^{-2}$  to determine the sensitivity of the results on this choice. Thus, as presented in Appendix I, while a choice of 400 m for the boundary mass produced overdamped conditions, very markedly slowing down the structural relaxation, a choice of  $4 \times 10^{-2}$  produced erratic results.

### III. RESULTS

#### 3.1 Time Dependent Changes in Structural Properties

The time dependent changes in several ensemble average intensive structural properties for a period of 200 atomic fluctuations (4000 time steps) are shown in Figs. 1a-1g. Here, the period of an atomic fluctuation is taken as  $5.4 \times 10^{13} \text{sec}$ . (see (I), [4]). The figures show both the level of fluctuations in overall average properties, as well as their monotonic changes over this period, first, for the entire ensemble of 144 atoms, but also for the subensembles of Zr and Cu atoms, as marked. Among these, Fig. 1a shows the changes in the average Voronoi polygon volume per atom ( $r_0^2$  times area per atom). Clearly, the regular fluctuations due to the boundary mass are apparent - not only in the fluctuations of the volume, but to some extent in all other properties, as can be seen by inspection of Figs. 1b-1g. Figures 1b and 1c, e.g., show the corresponding changes in the ensemble average values of the enthalpy and site distortion parameter <sup>2</sup>, while Figs. 1d-1g give the related changes in the atomic site pressure, maximum shear stress (in the plane regardless of orientation), the  $xy$  shear stress, and the

<sup>2</sup>For definitions of these intensive parameters describing structural properties of the glassy state, refer to (II)[5].

atomic site bulk modulus – all averaged over the entire ensemble as well as over only the Zr atoms and the Cu atoms, as indicated in the figures. The averaging has been done for every fluctuation, i.e., after every 20 time steps without any smoothing. Clearly, as stated above, the major and regular fluctuations with a period of about 18 atomic fluctuations is due to the border mass and must be ignored. When these are discounted, there is a clear trend of decrease in the volume, enthalpy, and site distortion. Large local fluctuations, however, remain particularly in the atomic level stresses and local bulk moduli. Additionally, it is evident that the atomic site pressures, maximum shear stresses, and bulk moduli for the Zr atoms, are much larger than the average, while the reverse is true for the Cu atoms. As already noted in (II), this is a direct result of the stiffer environment of the Zr atom than that of the Cu atom. The effect of this on the enthalpy fluctuations is in the reverse order, where as must be the case, more energy is stored, on the average, in the more compliant surroundings of the Cu atoms. Furthermore, it can also be observed that in the regular oscillations of the boundary mass, the fluctuations of the Voronoi volume and the atomic pressure are out of phase, i.e., as the atomic site pressure increases, the local volume decreases, and the atomic site bulk modulus increases. This direct response of the local site properties under the action of the boundary mass, however, does affect the kinetics of structural relaxation by speeding it up to some extent (see Appendix I). We note from Figs. 1a-1g that there are substantial reductions in excess properties (over and above those of an ordered hexagonal crystal) in enthalpy, local volume per atom (Voronoi volume), and site distortion over the total relaxation span of 200 fluctuations. There is a corresponding increase in

the local bulk moduli from 17 to about 18 (in units of dimensionless pressure) or by an amount of 6%. In comparison, there are no important relaxations in the atomic level pressures and maximum shear stresses. Since the changes in enthalpy must come from the reduction in root mean square elastic strain energies, however, it must be concluded that the observed changes come about primarily from the increases in bulk modulus and a corresponding increase in atomic level shear moduli. Although all ensemble average properties fluctuate considerably, the ratio of the average fluctuation amplitude to the current average level of the property shows large differences between different properties. These ratios are listed in Table I and indicate that initially, the ratios are largest for the atomic pressure and shear stress, while they are comparatively low for the atomic volume. Over the simulation span, however, the fractional changes in the atomic volume exceed those in the stresses. It is also interesting to note that although the change in the average levels of the atomic stresses are quite small, they are very substantial in the amplitudes of fluctuation. The source of these differences are clear. Thus, while the fluctuations and changes in the atomic volume are quite small on the absolute scale, being limited by the overall level of free volume that can be squeezed out, the stresses can fluctuate between large negative to large positive values about an equilibrium level in response to only small displacement amplitudes. To concentrate attention more specifically on the actual fluctuations, unaffected by the superimposed large fluctuations produced by the boundary masses, the root mean square deviations from the current ensemble average values in the structural parameters were determined after each atomic fluctuation (for every 20 time steps) according to the formula

$$X_{rms} = \langle (X(i) - \langle X(i) \rangle_t)^2 \rangle_t^{1/2} . \quad (2)$$

In Eqn. (2), the brackets mean ensemble averages either over the entire population or over only the Zr and Cu atoms, and  $t$  indicates that the information is evaluated at a given time (after every 20 time steps). The results of this type of evaluation are given in Figs. 2a-2g, paralleling the results given in Fig. 1. These results show some of the same effects shown in Fig. 1. The fluctuations now do not show the overwhelming pulsation resulting from the boundary mass. There is a clear and perceptible decrease in the fluctuations in the atomic volume and the site distortion parameter over the simulation span. Since the average levels for the fluctuations of the Zr atoms differs markedly from that of the Cu atoms, the root mean square fluctuations in either of these atoms is less than that over the entire ensemble for most of the properties, by virtue of the mode of the overall ensemble averaging procedure.

### 3.2 The Kinetics of Structural Relaxation

Much experimental research on structural relaxation in amorphous media, in common with stress relaxation and internal friction, has established that such relaxations are not simple mono-energetic processes characterizable by a single relaxation time. It has instead been proposed by many researchers that the relaxations in an amorphous solid are distributed in relaxation time, or in a somewhat more fundamental variant, that they are distributed in activation

energy and frequency factor. In this point of view, which we have taken earlier [8,9], in a narrow range of observation, the relaxation of any property can be characterized by a simple exponential given by:

$$\psi_i(t) = \frac{X_i(t) - X_i(\infty)}{X_i(o) - X_i(\infty)} = \exp\left(\frac{-t}{\tau_i}\right), \quad (3)$$

where  $\psi_i(t)$  is the level of the normalized property at time  $t$  of an element  $i$  and  $X_i(t)$ ,  $X_i(o)$ , and  $X_i(\infty)$  are the actual values of the property at time  $t$ , at the beginning of relaxation and at the end of relaxation, respectively, when equilibrium is reached. Since the relaxation is a thermally activated process, it is expected to have a characteristic relaxation time  $\tau_i$ , given by:

$$\tau_i = \tau_{i_0} \exp\left(\frac{\Delta H_i}{kT}\right), \quad (4)$$

where  $\Delta H_i$  is an activation enthalpy over the key barrier holding back the local relaxation and  $1/\tau_{i_0}$  is a fundamental frequency factor. It is then stated further that if the observation is not in a narrow range, but spans over many decades in time, or alternatively is accomplished over a span in temperature, other, both easier and more difficult relaxation processes with shorter or longer relaxation times become also observable. This requires a superposition of many processes that are continuously distributed in relaxation time  $\tau$ , according to a charac-

teristic and structure dependent normalized distribution function  $p(\tau)$ , to result in

$$\psi(t) = \int_0^{\infty} p(\tau) \exp(-t/\tau) d\tau, \quad (5)$$

and obeying the normalization condition

$$\int_0^{\infty} p(\tau) d\tau = 1. \quad (6)$$

Many procedures of operational inversion have been advanced [10-13] for the determination of such distribution functions from experimental data collected over long periods of time or over different temperatures. On the other hand, based on quite successful empirical procedures dating back to Kohlrausch [14], more than a century ago, a different approach has been suggested to the accounting for the non-exponential form of the long term relaxation behavior of amorphous media. In this approach, recently revived by Williams and Watts [15], it is observed that the relaxation in the normalized property can be fitted quite well over a relatively wide range of time to a modified relaxation function with a fractional exponent given as:

$$\psi(t) = \exp\left(\frac{-t}{\tau_w}\right)^\beta \quad (7)$$

where  $\tau_w$  is a new relaxation time and  $\beta$  is usually in the range of 0.5. While many recent investigators have adopted this form of presentation on the basis of its simplicity, and have asserted that it reflects a more complex non-Arrhenian relaxation, others have searched for a common denominator between the physically more appealing, but operationally more complex form given above in Eqn. (5) and the simpler form given by Eqn. (7) [16,17]. Thus, the stretched exponential form of Kohlrausch has been found consistent with a random walk of thermally activated diffusion of some impotent configurations to a central site, where upon arrival, a measurable unit relaxation event takes place. The fractional exponent then arises from a distribution of free energy barriers in the preparatory diffusion process of the key impotent configurations to the central site where they trigger the unit relaxation process. To obtain the fractional power  $\beta$  in the exponent of the exponential, it has been necessary to assume special distributions of barrier energies with exponential tails. Operational procedures have been developed further to obtain distribution functions of barrier heights in the diffusion problems from experimental data directly [18].

We consider these two different points of view as alternative operational approaches to represent the same physical phenomenon, in which the relaxation process is distributed in relaxation time or in activation energy and frequency factor. Whether the actual unit relaxation process is a sudden transformation of a local configuration from a more open one to a more compact one in one thermal fluctuation, or is composed of a series of prior impotent diffusive steps

approaching a central site without any observable effect, finally triggering the observable unit relaxation process upon arrival at this site is difficult to decide. The topological details of the simulation described in some detail in (II) [5] indicate that in reality, the processes may be a combination of both pictures, where the central unit process is noted to be the dissolution of 5 and 7 sided polygon dipoles. Noting difficulties in relating the Williams-Watts relaxation function uniquely to distribution functions of energies in preparatory diffusive processes [18], or performing an operational inversion to calculate  $p(\tau)$  from equations of the type given by Eqn. (5), we will merely adopt the Williams-Watts function and obtain the best fit of the results of our simulation to it. We justify this less than complete analysis by noting that the simulation covers only a very small portion of real time extending over only 200 atomic fluctuations, making it virtually impossible to obtain any relaxation times that are comparable with experimental information.

The results of fitting the ensemble averages of the evolving structure parameters presented in Fig. 1a-1g to the Williams-Watts function are given in Figs. 3a-3g. In these figures, the overall ensemble averages are shown by the fluctuating form. The best fit to the Williams-Watts function is given by the smooth solid curve to determine the exponent  $\beta$  and time constant  $\tau_w$ . Finally, the dotted curves, also shown on many of the plots, represent the best fit to the simple relaxation function with  $\beta = 1$  (Eqn. 3). The resulting best fit constants for the Williams-Watts relaxation function are given in Table II. We note from here that the relaxation of atomic volume, enthalpy, and site distortion are all characterizable with nearly the same function having a relaxation time  $\tau_w$  in the

vicinity of 7 fluctuations (= 140 time steps) and an exponent of  $\beta = 0.5$ . The relaxation of the shear modulus obeys nearly the same form of the equation with, however, a relaxation time of more than twice the length. In comparison, the relaxation of atomic site pressures and maximum shear stress are much slower, as is apparent from Fig. 1, and is characterizable by a very much longer time constant of around 53 fluctuations (= 1060 time steps) and a considerably larger exponent of  $\beta = 0.85$  coming close to the simple relaxation process of Eqn. (3).

Examination of Figs. 3a-3g show that all ensemble properties decrease from quenched-in initial excess values to lower values during the simulation span of 200 fluctuations. The decreases are more dramatic and substantial for volume per atom, site distortion parameter, and enthalpy than they are for the individual stresses. The ensemble averages of atomic site shear moduli actually increase, as they should. The decrease in the atomic site pressure is 3%, while that in atomic site maximum shear stress is 5%. The related rise in the atomic site shear modulus is 5%, while the rise in the atomic site bulk modulus could be determined to be 6% from the information given in Fig. 1g. The corresponding decreases in the ensemble average enthalpy is 14%, that for the volume per atom is 10%, and for the site distortion parameter only 2%. Considering that the ensemble average fractional change of enthalpy must be predominantly coming from the change in internal strain energy stored partly in shear strain energy and partly in bulk compression strain energy, we estimate the fractional enthalpy change from

$$\frac{\Delta h}{h} \simeq \Delta \ln \left( \frac{p^2}{2K} + \frac{\tau^2 max}{2\mu} \right) \Omega, \quad (8)$$

where  $K$  is the bulk modulus and  $\mu$  the shear modulus. Evaluations of Eqn. (8) gives for  $\Delta h/h$  exactly 14 % from the changes in pressure, maximum shear stress, bulk modulus, shear modulus, and atomic volume. We consider this as a good check on internal consistency in the simulation.

We note further, in passing, that the ratio of the ensemble average maximum shear stress to shear modulus is 0.21, while the corresponding ratio of average pressure to bulk modulus is 0.085. These are both somewhat higher than the ratios reported by Egami and Vitek [19] for a three-dimensional amorphous medium. We attribute the difference to the two-dimensional nature of our material.

Since the relaxation of most of the properties, except the atomic site stresses, can be characterized by a Williams-Watts function with a fractional exponent of 0.5 and a characteristic time constant  $\tau_w = 7$  atomic fluctuations (= 240 time steps), it is possible to give a distribution function  $p(\tau)$  of relaxation times of simple Arrhenian processes on the basis of an analytical solution of the integral equation obtained by equating Eqns. (5) and (7). This solution, obtained by Lindsay and Patterson [18], gives:

$$p(\tau) = \frac{1}{2\tau_w} \sqrt{\frac{\tau_w}{\pi\tau}} \exp\left(\frac{-\tau}{4\tau_w}\right). \quad (9)$$

For comparison with experimental results obtained by Deng and Argon [8], we convert this distribution into one of activation free energies  $\Delta G^*$  by noting that

$$p(\Delta G^*) d\Delta G^* = p(\tau) d\tau = p\left(\frac{\Delta G^*}{E_o}\right) d\left(\frac{\Delta G^*}{E_o}\right), \quad (10)$$

giving

$$p\left(\frac{\Delta G^*}{E_o}\right) = E_o p(\Delta G^*) = E_o p(\tau) \frac{d\tau}{d\Delta G^*}. \quad (11)$$

Upon introduction of the relations

$$\left(\frac{\tau}{\tau_w}\right) = \left(\frac{\tau_G}{\tau_w}\right) \exp\left(\frac{\Delta G^*}{kT}\right), \quad \therefore \tau_G = 1/2\pi\nu_G. \quad (12a, b)$$

into Eqns. (9)-(11) it is found that:

$$p\left(\frac{\Delta G^*}{E_o}\right) = \left(\frac{E_o}{kT}\right) \frac{l}{2\sqrt{\pi}} \sqrt{\left(\frac{\tau_G}{\tau_w}\right) \exp\left(\frac{\Delta G^*}{E_o}\right) \left(\frac{E_o}{kT}\right)}$$

$$\exp\left\{-\frac{1}{4} \left(\frac{\tau_G}{\tau_w}\right) \exp\left(\frac{\Delta G^*}{E_o}\right) \left(\frac{E_o}{kT}\right)\right\}, \quad (13)$$

where  $\nu_G$  is a fundamental atomic cluster frequency related to the clusters which undergo structural relaxations. Noting that for the simulation  $kT/E_o = 0.1$ , and taking  $\nu_G$  as the atomic frequency,  $\tau_G/\tau_w = 1/14\pi$  for  $\tau_w = 7\tau_G$ , as obtained from Table II, it is possible to evaluate the distribution function of Eqn. (13) as a function of  $\Delta G^*/E_o$ . The result of this is given in Fig. 4. While the shape of this figure compares favorably with that obtained by Deng and Argon [9] from internal friction measurements in a  $Cu_{59}Zr_{41}$  alloy (their Fig. 8), the energy scale of the latter is a factor of 26.8 larger than the simulation results. This is not surprising, since the frequencies in the internal friction results were in the range of  $0.25 H_z$ , while those in the simulation were no smaller than  $10^{11} H_z$ .

### 3.3 Inhomogeneities and Clustering of Atomic Motions

Figures 5a and 5b show the total atom motions in two separate time periods of 10 fluctuations each (5a from 70-80; 5b from 100-110). The displacements, at a magnification of 10, are shown as bars emanating from the initial positions of the atoms at the beginning of the time period. The motions shown in these two frames are typical of many such frames that have been examined. In Fig. 5a, the motions are relatively random over most of the field, except in the central upper portion, where group-like displacements toward the left are evident. In Fig. 5b, on the other hand, very large group-like motions of atoms toward the left are visible in the entire right half of the simulation cell. Such large to and fro motions of blocks of atoms often reversed in the following 10 fluctuations. They are attributed to the resonances resulting from the boundary mass that show up clearly in the pulsations of the volume shown in Fig. 1a and were therefore, largely ignored.

More importance was attached to the clustering of the atomic structure parameters, which were considered to be more genuine and were followed in some detail. Figures 6a-6c show the clustering of enthalpy, volume per atom, and site distortion parameter averaged over the entire simulation span of 200 fluctuations. The length of the solid horizontal bars reflect the relative magnitudes of the respective properties. All the atomic site properties that have been encircled, are larger than the ensemble average, except those in circles 3 and 5, which are smaller than the ensemble average. The bars emanate from the centers of atoms. The atoms bearing numbers are thus either in the upper or lower 10

percentile of the population with largest and smallest properties. Clustering in atomic level pressure, maximum shear stress,  $xy$  shear stress, and shear modulus, or bulk modulus was less prominent. For these, the excess properties which were also large were, however more uniformly mixed. These clusters in enthalpy, volume per atom, and site distortion indicate that excess properties in the field have often long life times and persist through even relatively long simulation spans. If they are to represent actual structural relaxations in real time, they must, of course, have life times that must be larger by orders of magnitude than the period of 200 fluctuations considered here. The evolution of properties in clusters and their random changes in size and shape was followed in more detail over smaller increments of the simulation span, but maps of these changes will not be presented here. From examination of these changes, however, the following important observations have been made:

- a. Prominent clustering occurs only in excess enthalpy, volume per atom (free volume), and site distortion. These are also the properties that, as shown in Figs. 1 and 2 show the more prominent relaxation effects.
- b. Clustering of atomic level stress is slight. The largest clusters of atoms with excess pressure or excess maximum shear stress were only 2-3 atoms across. Generally, it was found that atoms under large stress of all types, i.e., pressure, or maximum shear stress were the Zr atoms, while those under the lowest pressure or shear stress were the Cu atoms. Since these were initially randomly spaced, and since the simulation time spans were too short to produce much chemical short range ordering, the lack of clustering is not surprising. As already noted, the clustering correlates with

more prominent relaxation strength. Somewhat similar observations were made also by Maede and Takeuchi [20] in their study of radial correlation functions of the atomistic structure parameters, but they did not give a cause.

- c. Comparison of the clustering in Figs. 6a-6c shows that the clusters with high excess enthalpy tend to overlap with clusters having high excesses of free volume, and those showing excesses of site distortion. Parenthetically, it must be observed that clustering of excess enthalpy requires clustering of a combination of dilatational and shear strain energy, which, however, does not require clustering of either pressure or maximum shear stress.
- d. Relief of site distortion in clusters of this property resulted in clustering of shear strains of random sign shown in Fig. 6d, which showed spatial correlation with the clusters of site distortion. A similar correlation was found between the relief of excess free volume and volumetric compaction.
- e. Some spatial correlation was found between local shear strain production during relaxation and increments in positive dilatation. Such dilatancy is known to be a prominent effect during imposed shear strains. The importance of this effect is more clearly demonstrated in the comparison study (IV) of simulation of plastic shear deformation [16].
- f. It was found generally that regions with excesses of free volume coincided with regions with reduced bulk modulus, or shear modulus, or both, while the opposite was true for regions of deficiency of free volume. This is considered to be an important source of distribution in frequency factor

found by Deng and Argon [9] in internal friction experiments in  $Cu_{59}Zr_{41}$  glasses.

- g. Comparison of the clustering of site distortion with distributions of Voronoi polygons with sides other than six reported in the companion study (II) [5], showed a necessary correlation between large distortions and non-hexagonal polygons.

In summary of the above observations, we note that three types of clusters were observed: an excess volume cluster (free volume), called an  $n$  cluster by Egami and Vitek [19], has a lower local pressure and a lower local modulus; a cluster of deficiency of volume, called a  $p$  cluster by Egami and Vitek, which possesses a higher local pressure and a higher local modulus; and finally, a site distortion cluster, which possesses a higher level of maximum shear stress and also an excess of volume. Only the first and third types of cluster undergo important evolution during structural relaxation, while the first contracts the third undergoes a combined shear and dilatation. The changes in the  $p$  type cluster are far less consequential or apparent.

The evolution of properties in 5 clusters were studied in more detail as a function of time during the simulation. These, marked 1-5 in Figs. 6a and 6c, each contain roughly equal numbers of Zr and Cu atoms. Cluster 1 possessed a substantial excess of volume per atom in the initial state. Clusters 2 and 4 possessed a large excess in site distortion, while clusters 3 and 5 had quite low levels of excess volume per atom. The changes in volume per atom, enthalpy, site distortion, atomic site pressure, maximum shear stress, atomic site shear

modulus, are shown as a function of time of simulation in Figs. 7a-7f. We note from examination of these traces that cluster 1, which has the most extreme excesses in volume shows the most dramatic relaxations in volume, in enthalpy, in site distortion, in rise in pressure, and in rise in shear modulus, mostly by undergoing a decrease in dilatation. Clusters 3 and 5 with the minimum excesses in properties, show no important changes, but exhibit only flutter. Clusters 2 and 4, which had large initial site distortions, show larger variations in enthalpy, site distortion, pressure, and shear stress, but no systematic changes.

#### IV. DISCUSSION

Isothermal structural relaxations in real amorphous media at about half the glass transition temperature would be comparatively very slow processes. In metallic glasses such as the  $Cu_xZr_{1-x}$  glasses that have been simulated here, structural relaxations have characteristic time constants that are closely comparable to those found in anelastic relaxations [9] and have activation energies that span between 1-2 eV and frequency factors that are in the range of  $10^{10} - 10^{12} s^{-1}$ . This gives ranges in relaxation time from  $10s - 10^{13}s$ . Processes with such very long relaxation time can, of course, not be simulated by MD. Therefore, in the simulation reported here, rather artificial initial conditions were taken, in which an alloy at its melting point was quenched at infinite rate to a low temperature, where it had an extremely large excess of properties that could be relaxed. The time span in the relaxation that could be reasonably simulated consisted of only 200 thermal fluctuations at a temperature equal to 0.556 of  $T_g$ , i.e., over a period differing from the required real times by 10-11 decades. Consequently, the results

presented here cannot be compared directly with those of metallic glasses under any realistic conditions. Therefore, these results must be examined primarily for the qualitative information that they convey, for the chronological ordering of processes, and the time independent kinematics of structural relaxation. This is also apparent from the distribution function of activation energies for relaxation of excess enthalpy, volume per atom, and distortion that were calculated by matching a Williams-Watts relaxation function to the results of the simulation. The distribution function has a peak at  $\Delta G^*/E_o = 0.45$ . Since the scaling factor  $E_o = 0.15\text{eV}$ . for this simulation [4], the observed characteristic activation energy is  $0.068\text{ eV}$ . and not  $1.5\text{ eV}$ ., as is the case for the real  $\text{Cu}_x\text{Zr}_{1-x}$  alloy. Clearly, the only processes that can be relaxed over such short periods of time are those that appear in the simulation. Indeed, if this activation energy and its associated relaxation period of 7 fluctuations are taken as accurate, and a formal upward scaling of relaxation times to  $\tau_2 = 4$  seconds (a  $0.25\text{ Hz}$  internal friction experiment) at  $T = 0.556T_g$  of a  $\text{Cu}_{59}\text{Zr}_{41}$  glass having a  $T_g$  of  $741\text{K}$  is done, according to direct scaling relation of  $\Delta G_2^* = \Delta G_1^* + kT \ln(\tau_2/\tau_1)$  an activation energy of  $\Delta G_2^* = 1.05\text{ eV}$  is obtained, where  $\Delta G_1^* = 0.068\text{eV}$ ,  $\tau_1 = 7 \times 5.4 \times 10^{-13}\text{sec}$ . and  $T = 412\text{K}$  have been used from the simulation. This is almost exactly the lowest energy in the spectrum of energies measured in internal friction experiments by (at  $0.25\text{ Hz}$ ) by Deng and Argon [9], that can produce relaxation at such a low homologous temperature. Thus, when properly scaled up, the results of the simulation are consistent also with experimental results. This however, implies a similarity in the shapes of the energy spectra at the atomic fluctuation scale with energies in the macroscopic scale for which no clear justification can

be furnished.

Considering the results of the simulation as a whole, we have shown that structural relaxations are complex and cooperative processes. The excess structural properties in the form of excess enthalpy, volume per atom (free volume), site distortion, atomic level stresses, and moduli are not uniformly spread out in the structure. The excess enthalpy, free volume, and site distortion show the greatest degree of clustering, while the atomic level stresses cluster less, since they are associated more directly with the Zr and Cu atoms, which were randomly distributed in the initial state of the structure. At the temperature of simulation ( $0.556T_g$ ), the relaxation is to a large extent a local and immobile one, i.e., the clusters with large excesses in properties show a decay in these by local atom motions. There were no important displacements of regions with large free volume toward regions with deficiencies in free volume, i.e., so-called  $n$  type clusters were not observed in any meaningful way to migrate to  $p$  type clusters, as described by Egami and Vitek [19] in their simulations. While such "interdiffusion" of defect clusters is very appealing, and may probably occur in more realistic situations in real time, they must require much longer periods of time, in excess of the simulation period studied here. We recall from the associated study (II [5]), that the topological features of the relaxation involve a reduction in the volume fraction of atom sites with 5 and 7 near neighbors, i.e., reduction of liquid-like boundary material by gradual dismemberment and dissipation of such regions, as they are replaced by a growth of quasi-ordered material consisting of atoms with 6 near neighbors. Our last associated study (IV) [6] demonstrated that it is this liquid-like boundary material, which seeds

shear transformations that are the principal modes of strain production in aged amorphous material before the ordered domains become large enough to permit plasticity by dislocation glide.

#### ACKNOWLEDGEMENT

The research reported here has received support from a number of different sources. The principal one of those was an NSF Grant No. DMR-85-17224. Other support, particularly for computations, came in the early phases from the Center of Materials Science and Engineering at M.I.T. from the basic NSF/MRL Grant DMR-84-18718, and in its final stages from the Defense Advanced Research Projects Agency under Contract N00014-86-K-0768. Additional salary support for DD was provided by the Allied Corporation through a fellowship, for which we are grateful to Dr. Lance Davis.

## REFERENCES

1. S. Takeuchi, K. Maeda, and S. Kobayashi, in "Amorphous Materials: Modeling of Structure and Properties", edited by V. Vitek (AIME: New York), P. 305 (1983).
2. S. Kobayashi and S. Takeuchi, J. Phys. F.: Met. Phys., **14**, 23 (1984).
3. S. Kobayashi, K. Maeda, and S. Takeuchi, Acta Met., **28**, 1641 (1980).
4. D. Deng, A.S. Argon and S. Yip (I), submitted to Acta Met.
5. D. Deng, A.S. Argon and S. Yip (II), submitted to Acta Met.
6. D. Deng, A.S. Argon and S. Yip (IV), submitted to Acta Met.
7. H.C. Andersen, J. Chem. Phys., **72**, 2384 (1980).
8. D. Deng and A.S. Argon, Acta Met., **34**, 2011 (1986).
9. D. Deng and A.S. Argon, Acta Met., **34**, 2025 (1986).
10. W. Primak, Phys. Rev., **100**, 1677 (1955).
11. A.S. Novick and B.S. Berry "Anelastic Relaxation in Crystalline Solids", (Academic Press: New York) (1972).
12. A.S. Argon, J. Appl. Phys., **39**, 4080 (1968).
13. A.S. Argon and H.Y. Kuo, J. Non-Cryst. Solids, **37**, 241 (1980).
14. F. Kohlrausch, Pogg. Ann. Phys., **119**, 352 (1863).

15. G. Williams and D.C. Watts Trans. Faraday Soc., **66**, 80 (1970).
16. M.F. Shlesinger and E.W. Montroll, Proc. Natl. Acad. Sci., (USA), **81**, 1280 (1984).
17. J.T. Bendler and M.F. Shlesinger, Macromolecules, **18**, 591 (1985).
18. C.P. Lindsey and G.D. Patterson, J. Chem. Phys., **73**, 3348 (1980).
19. T. Egami, and V. Vitek, in "Amorphous Materials: Modeling of Structure and Properties", edited by V. Vitek (AIME: New York), p. 127 (1983).
20. K. Maeda and S. Takeuchi, J. Phys. F.: Met. Phys., **12**, 2767 (1982).

**TABLE I. Ratios of Fluctuation Amplitudes to Average Levels in Structural Parameters over the Simulation Span**

| Parameter                | $(\Delta X/\bar{x})_{initial}$ |     | $(\Delta X/\bar{X})_{final}$ | % change |
|--------------------------|--------------------------------|-----|------------------------------|----------|
| Atomic pressure          | 1.07                           |     | 0.6                          | 44       |
| Atomic Max. Shear Stress | 0.8                            |     | 0.5                          | 38       |
| Atomic Bulk Modulus      | 0.57                           |     | 0.45                         | 21       |
| Atomic Volume            | 0.07                           |     | 0.03                         | 57       |
| Enthalpy/atom            |                                | 0.2 |                              |          |
| Distortion parameter     |                                | 0.1 |                              |          |

**TABLE II. Best Fit Values of Williams-Watts Distribution Parameters Determined from Relaxation Simulation**

| Structure Parameter   | $\beta$ | $\tau_w^{(*)}$ | $X_o$  | $X_\infty$ |
|-----------------------|---------|----------------|--------|------------|
| Atomic Volume         | 0.55    | 130            | 1.668  | 1.504      |
| Enthalpy              | 0.5     | 140            | -1.344 | 1.565      |
| Distortion parameter  | 0.55    | 150            | 1.082  | 1.060      |
| Atomic Pressure       | 0.85    | 1060           | 1.486  | 1.454      |
| At. Max. Shear Stress | 0.85    | 1020           | 0.968  | 0.916      |
| Shear Modulus         | 0.5     | 320            | 4.232  | 4.396      |

(\*) in time steps (=0.05 fluctuations)

## APPENDIX I

### Boundary Masses

To maintain the external pressure constant in MD simulations, Andersen [7] introduced another dynamic coordinate into the basic Lagrangian representing the equations of motion of the atoms in the simulation. The new coordinate  $Q$  representing the volume of the simulation cell then gives the modified Lagrangian:

$$L(\rho_i, \dot{\rho}_i, Q, \dot{Q}) = \frac{1}{2}mQ^{2/3} \sum_{i=1}^n \dot{\rho}_i \cdot \dot{\rho}_i - \frac{1}{2} \sum_{\substack{i \neq j \\ i}}^n \phi(Q^{1/3} \rho_{ij}) + \frac{1}{2}M\dot{Q}^2 - \alpha Q \quad (A-1)$$

where all quantities have been defined earlier in Section 2.2 of the text.

To minimize artifacts of unwanted resonances of the fictitious boundary masses and the atoms in the simulation cell, it is necessary to choose the boundary mass carefully, not to affect the kinetics of any process that is being simulated. The recommended procedure is to choose  $M$  in such a way that the period of the fluctuations of  $Q$  is approximately equal to  $Q^{1/3}$  divided by the speed of sound in the simulation cell. As discussed in Section 2.2, this criterion gave a boundary mass of 4 atom masses. Nevertheless, to explore the effect of the boundary mass on the results of the simulation, other values one hundredth of the chosen value and hundred times the chosen value were also used to determine the effect of the choice.

Figures A-1a - A-1c show the results of a relaxation simulation of the volume, enthalpy, and internal pressure for the three different boundary masses. Clearly, the responses to boundary masses of 0.04 and 400 give insufficient damping and erratic behavior or supercritical damping respectively during the period of simulation lasting 1000 time steps (50 fluctuations). The results for the boundary mass of 4 show rather regular oscillations in properties that were presented already above. These could be readily isolated and discounted when necessary.

## FIGURE CAPTIONS

- Fig. 1 Time dependent changes in ensemble averages over 200 fluctuations (= 4000 time steps): (a) volume per atom, (b) enthalpy, (c) site distortion parameter, (d) atomic level pressure, (e) atomic level maximum shear stress, (f) xy shear stress, (g) atomic site bulk modulus. Ensemble averages are given both for the entire population as well as for the Zr and Cu atoms separately.
- Fig. 2 Time dependent changes in root mean square deviations from the ensemble mean values over 200 fluctuations: (a) volume per atom, (b) enthalpy, (c) site distortion parameter, (d) atomic level pressure, (e) atomic level maximum shear stress, (f) xy shear stress, (g) atomic site bulk modulus.
- Fig. 3 Best Williams-Watts function fits to the changes in ensemble averages for the same seven structure parameters given in Figs. 1 and 2.
- Fig. 4 The free energy barrier distribution function for the structural relaxations, obtained from the Williams-Watts distribution function by an operational inversion.
- Fig. 5 Two different states of incremental atom displacements during the simulation: (a) for the period between 70-80 fluctuations, (b) for the period between 100-110 fluctuations.
- Fig. 6 Field of excess properties averaged over the entire simulation period: (a) volume per atom, (b) enthalpy, (c) site distortion parameter, (d)

relaxation shear strains.

**Fig. 7** Time dependent changes of the structure parameters in five selected clusters: (a) volume per atom, (b) enthalpy, (c) site distortion, (d) atomic site pressure, (e) atomic site maximum shear stress, (f) atomic site shear modulus.

**Fig. A1** Effect of choice of boundary mass on the relaxation of excess properties: (a) volume per atom, (b) enthalpy, (c) atomic site pressure.

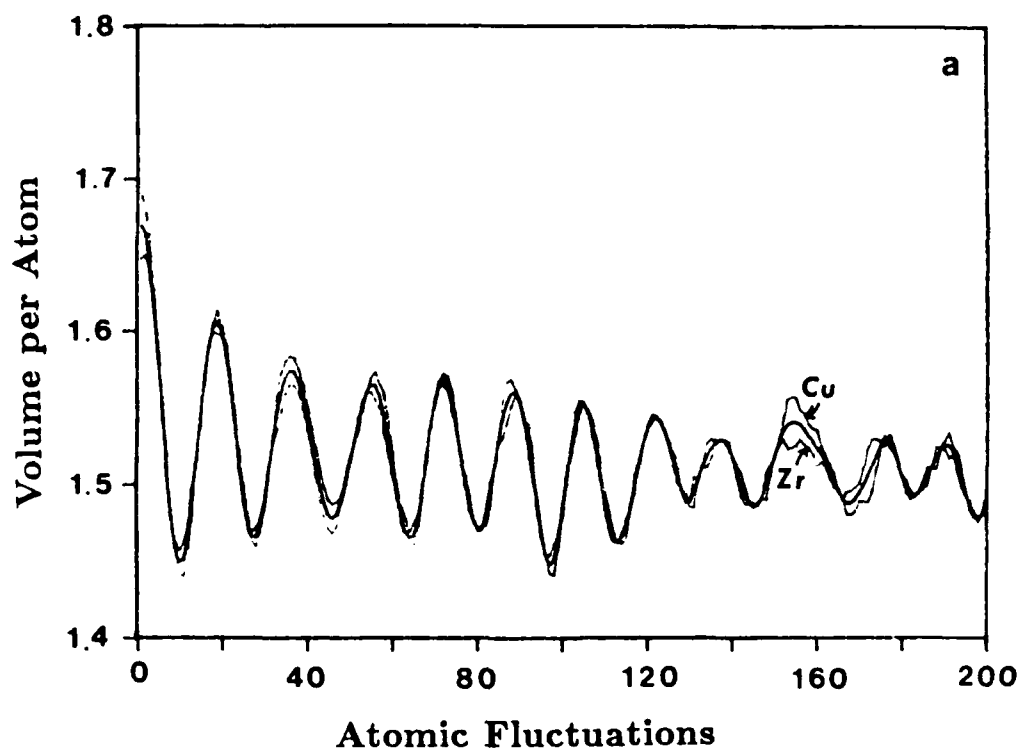


Fig. 1 Time dependent changes in ensemble averages over 200 fluctuations (= 4000 time steps): (a) volume per atom, (b) enthalpy, (c) site distortion parameter, (d) atomic level pressure, (e) atomic level maximum shear stress, (f) xy shear stress, (g) atomic site bulk modulus. Ensemble averages are given both for the entire population as well as for the Zr and Cu atoms separately.

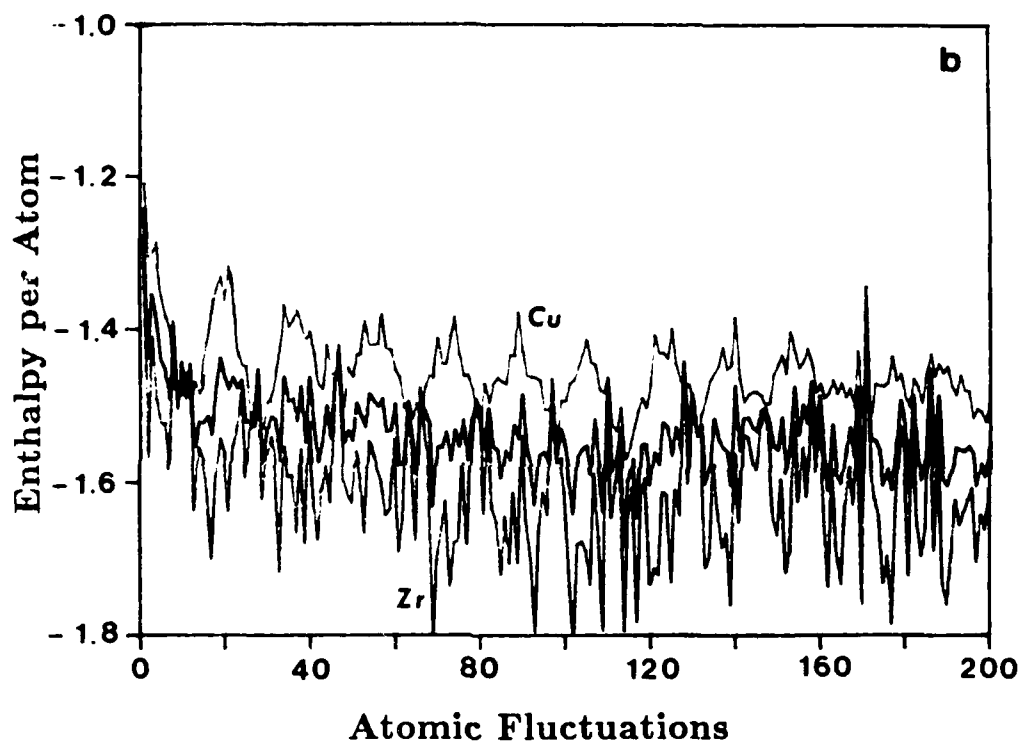


Fig. 1b

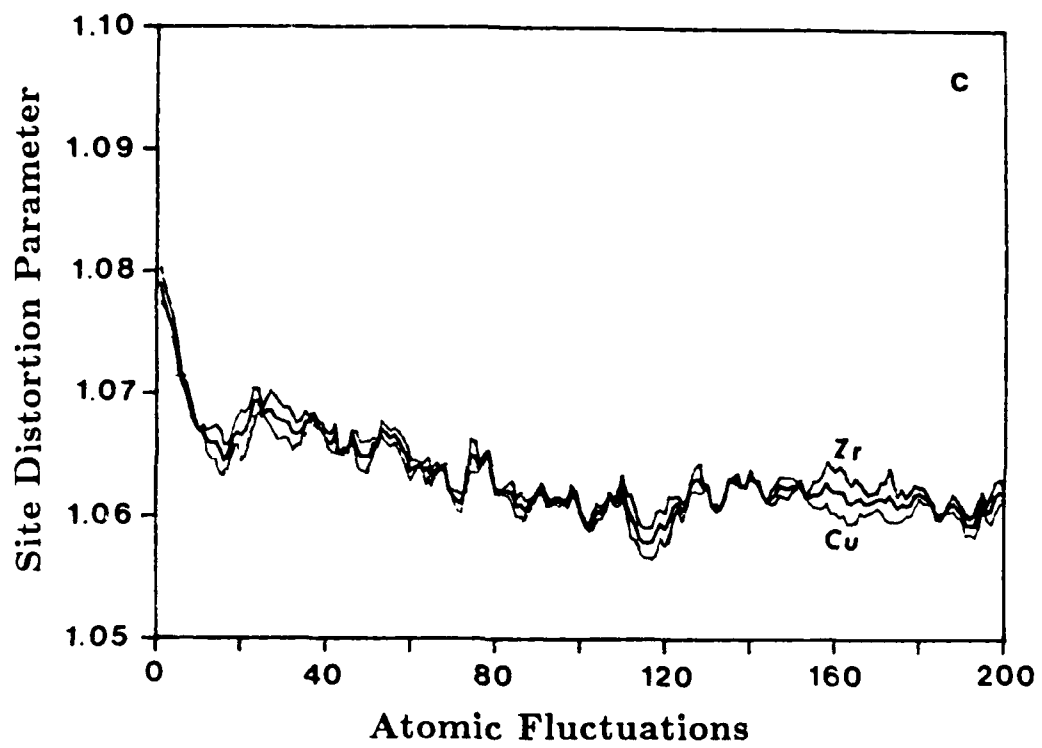


Fig. 1c

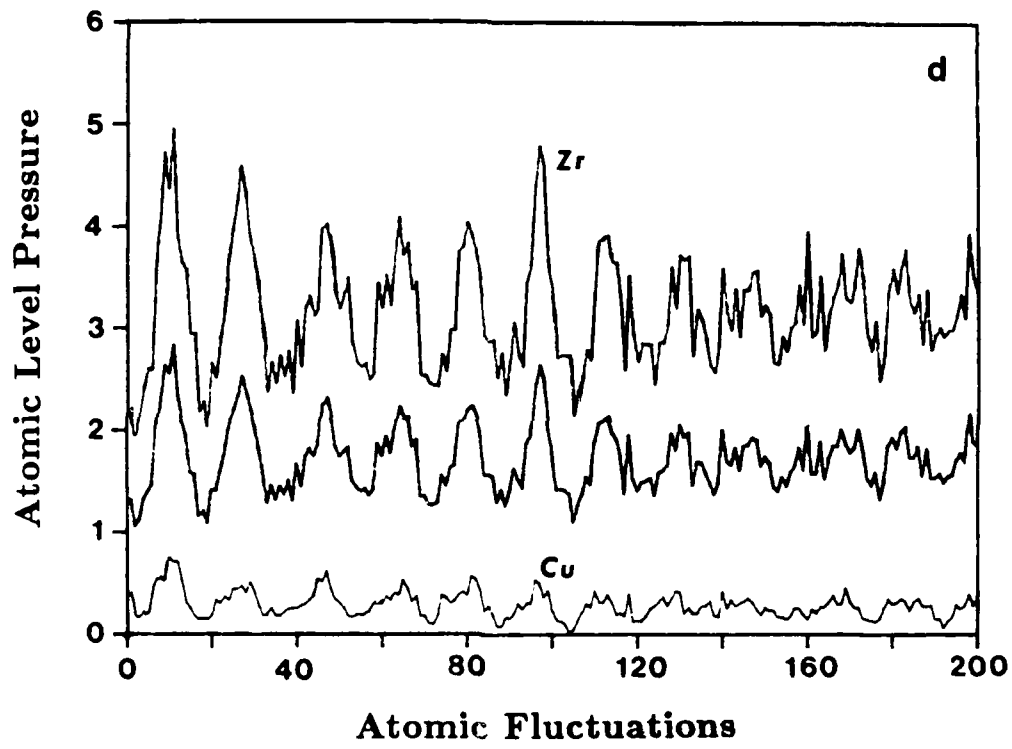


Fig. 1d

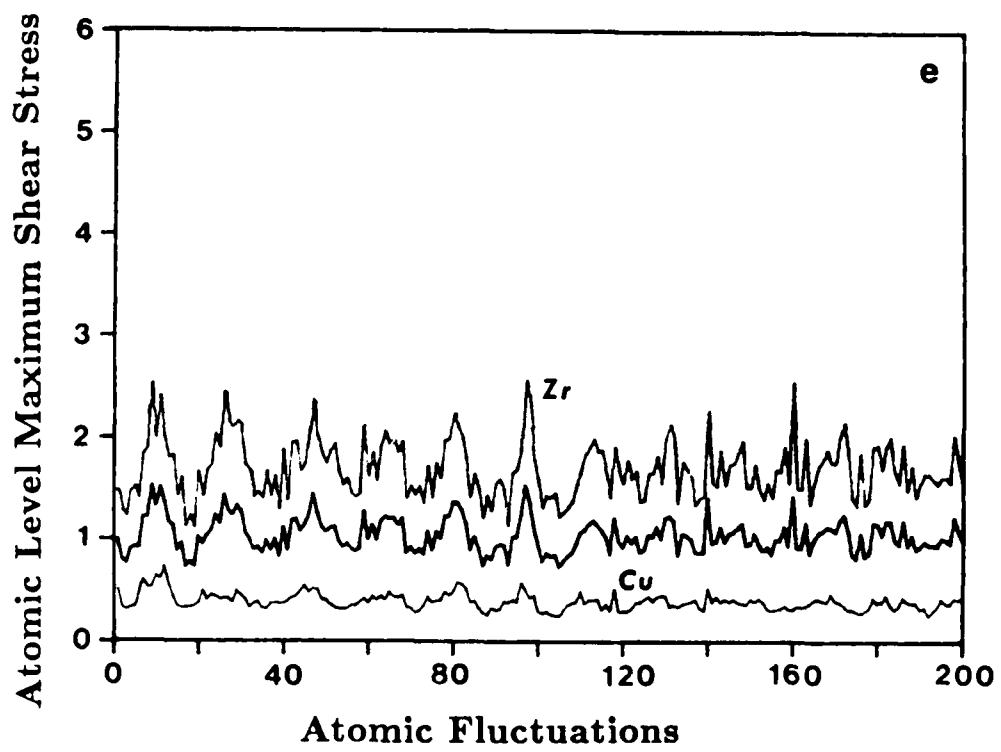


Fig. 1e

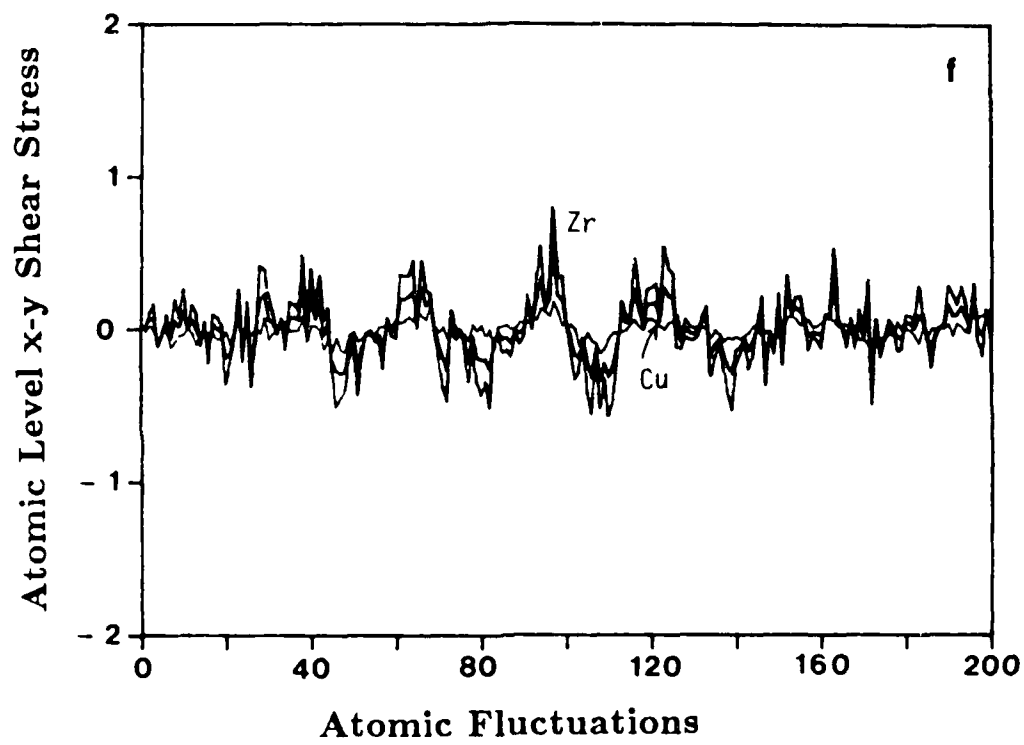


Fig. 1f

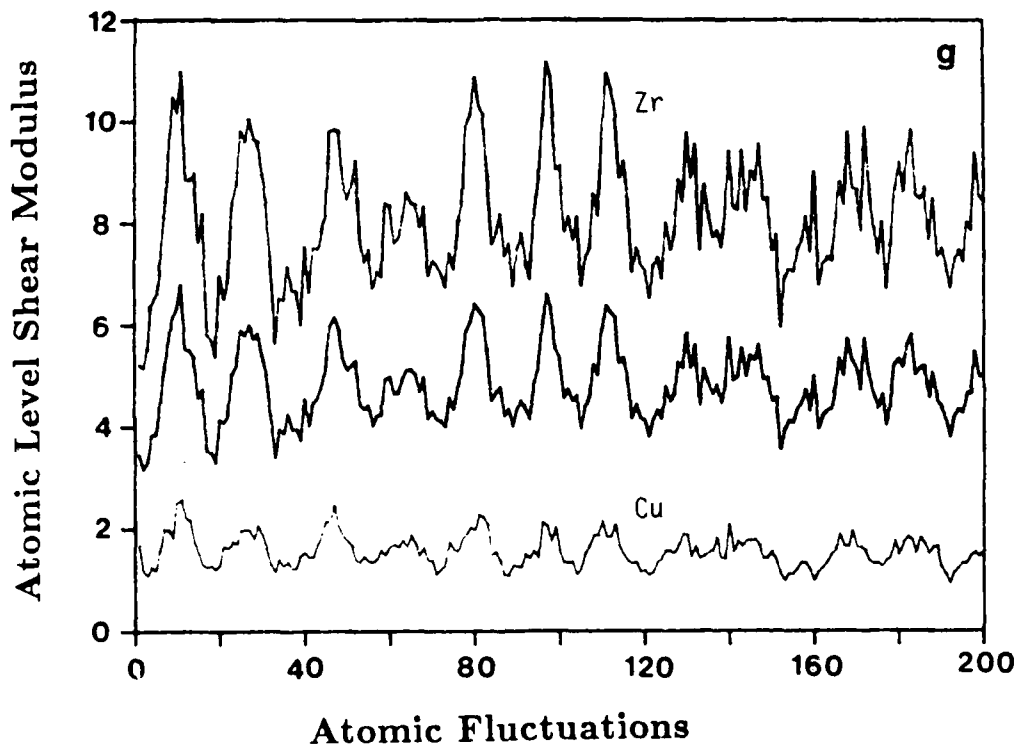


Fig. 1g

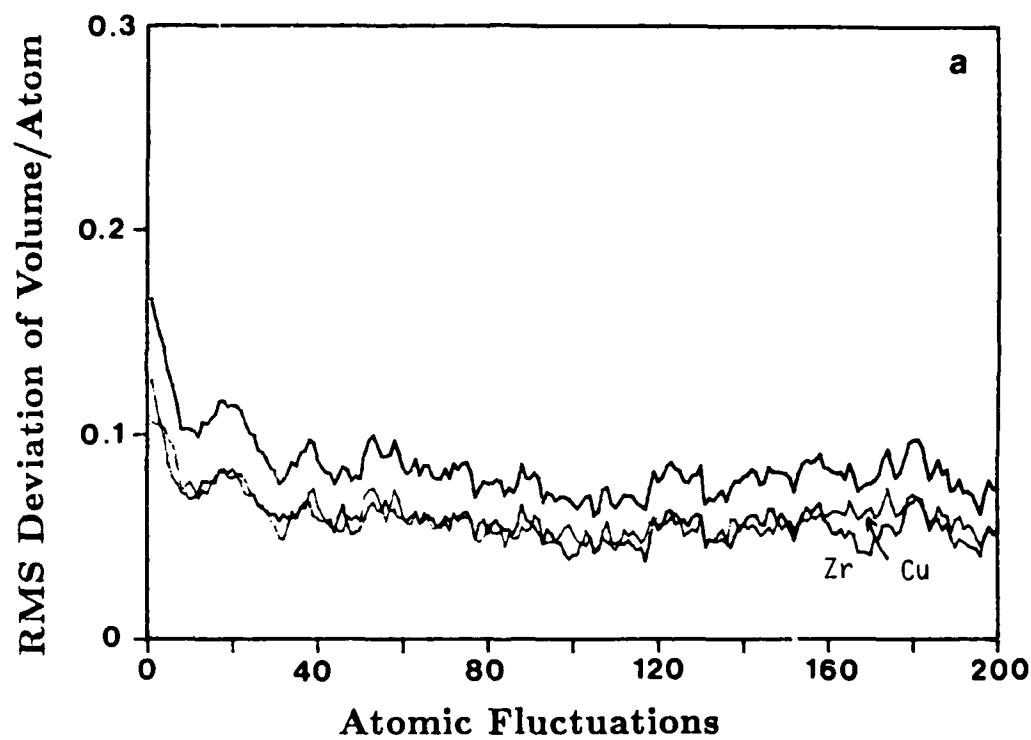


Fig. 2 Time dependent changes in root mean square deviations from the ensemble mean values over 200 fluctuations: (a) volume per atom, (b) enthalpy, (c) site distortion parameter, (d) atomic level pressure, (e) atomic level maximum shear stress, (f) xy shear stress, (g) atomic site bulk modulus.

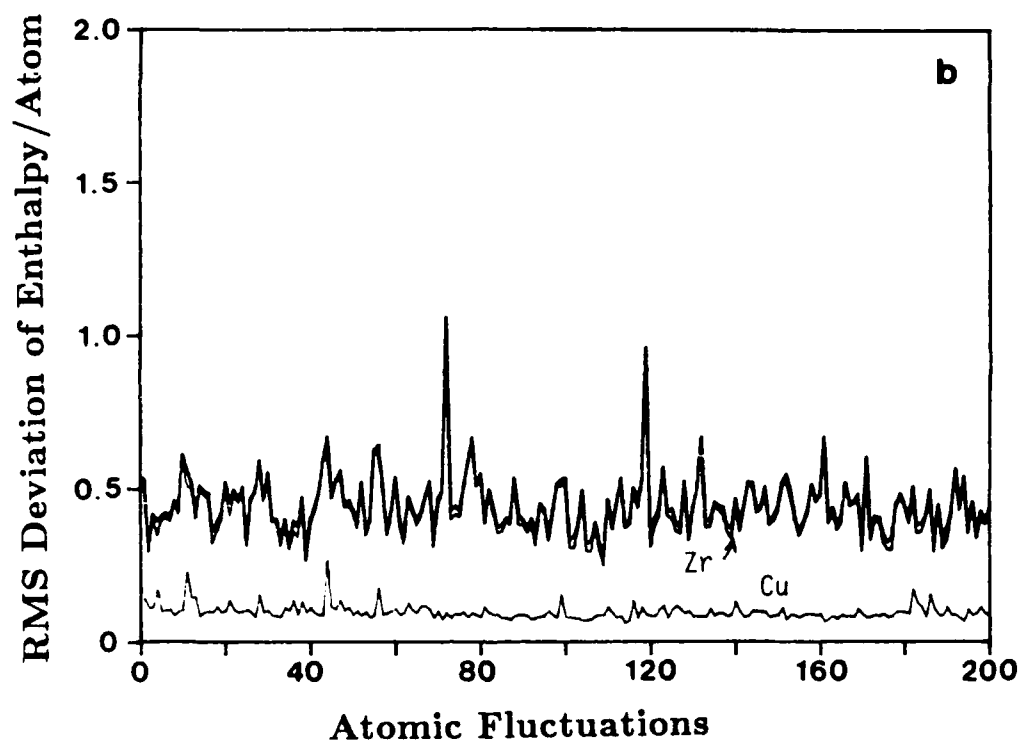


Fig. 2b

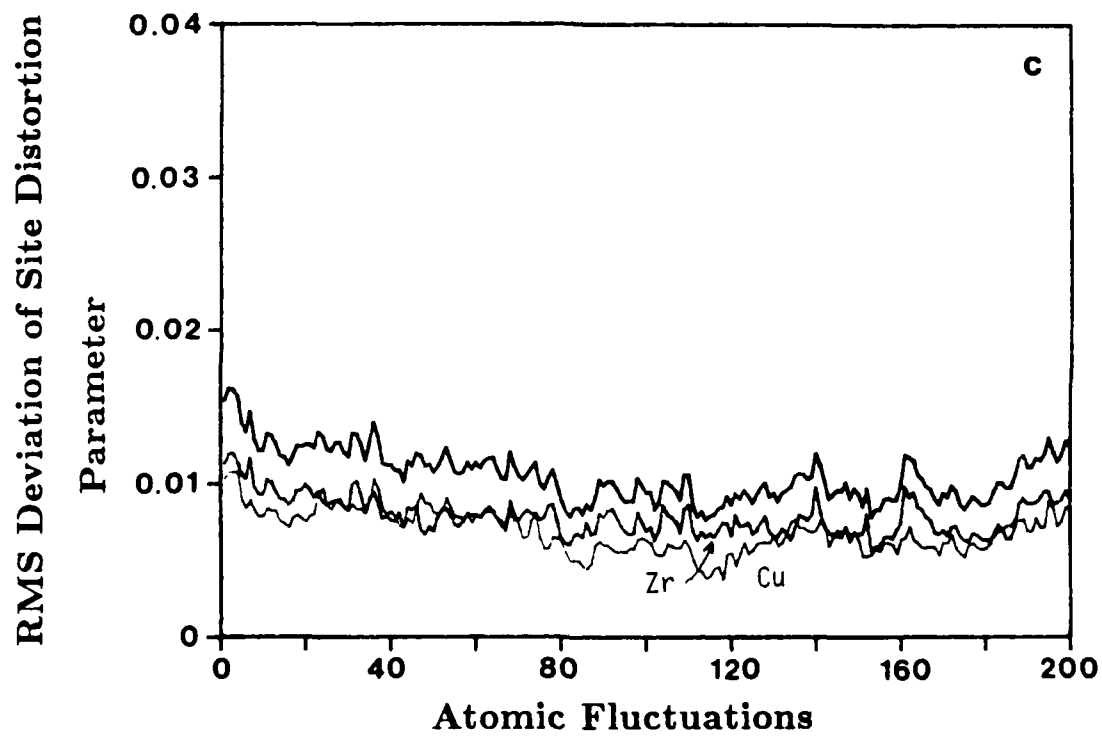


Fig. 2c

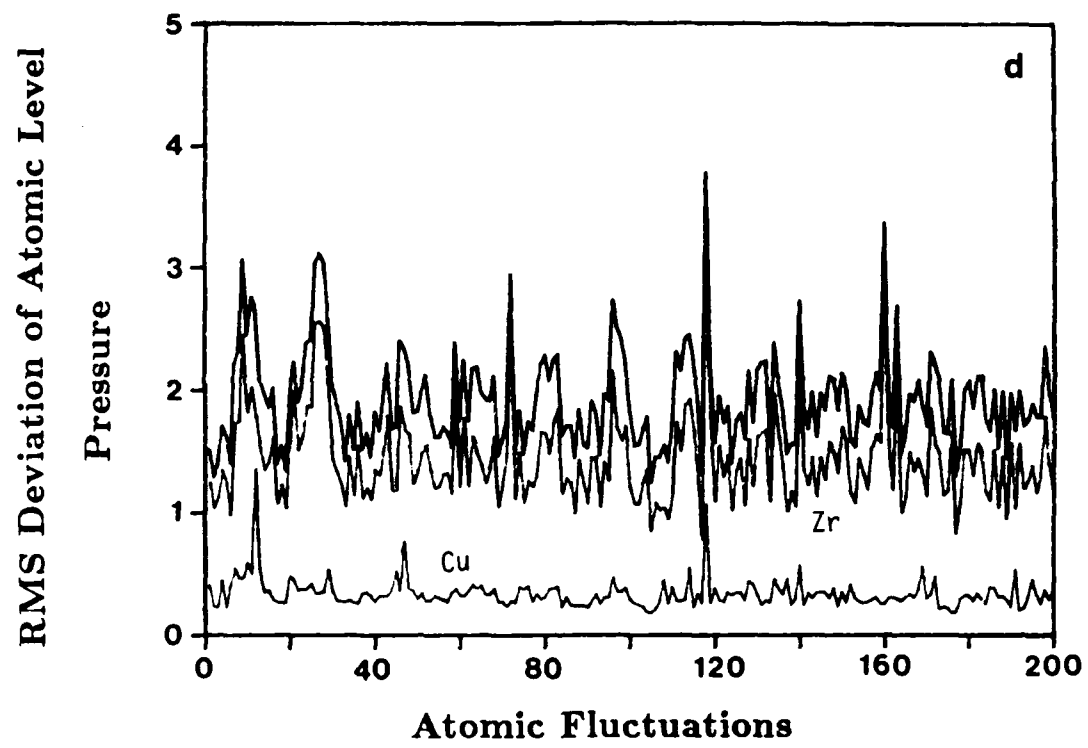


Fig. 2d

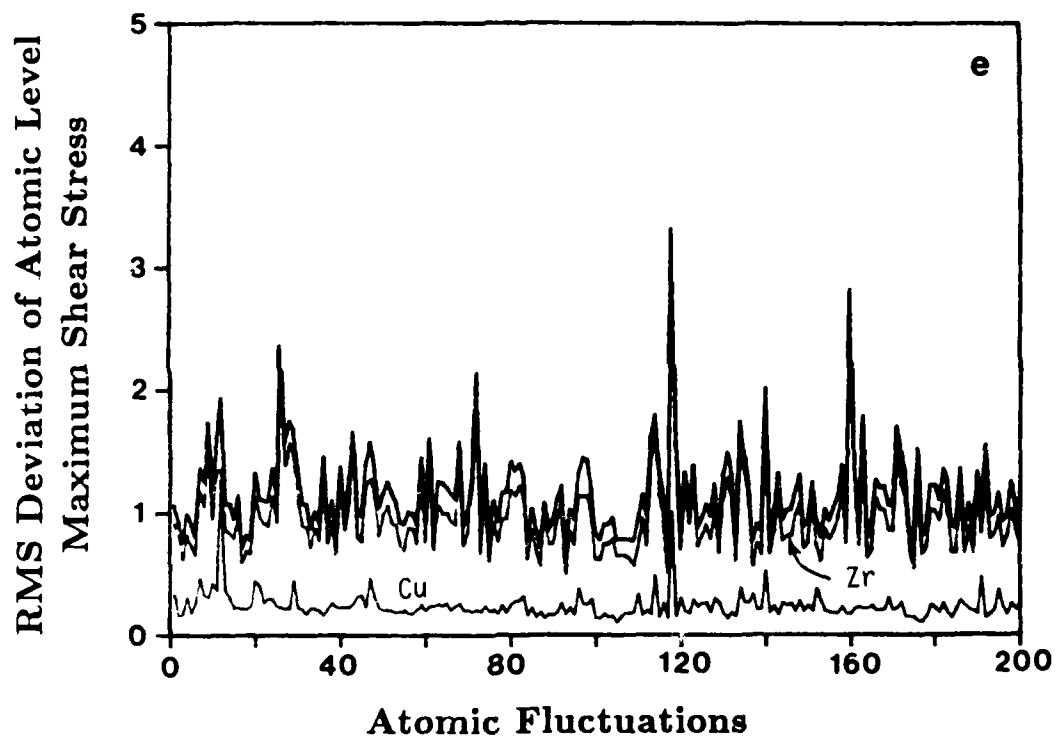


Fig. 2e

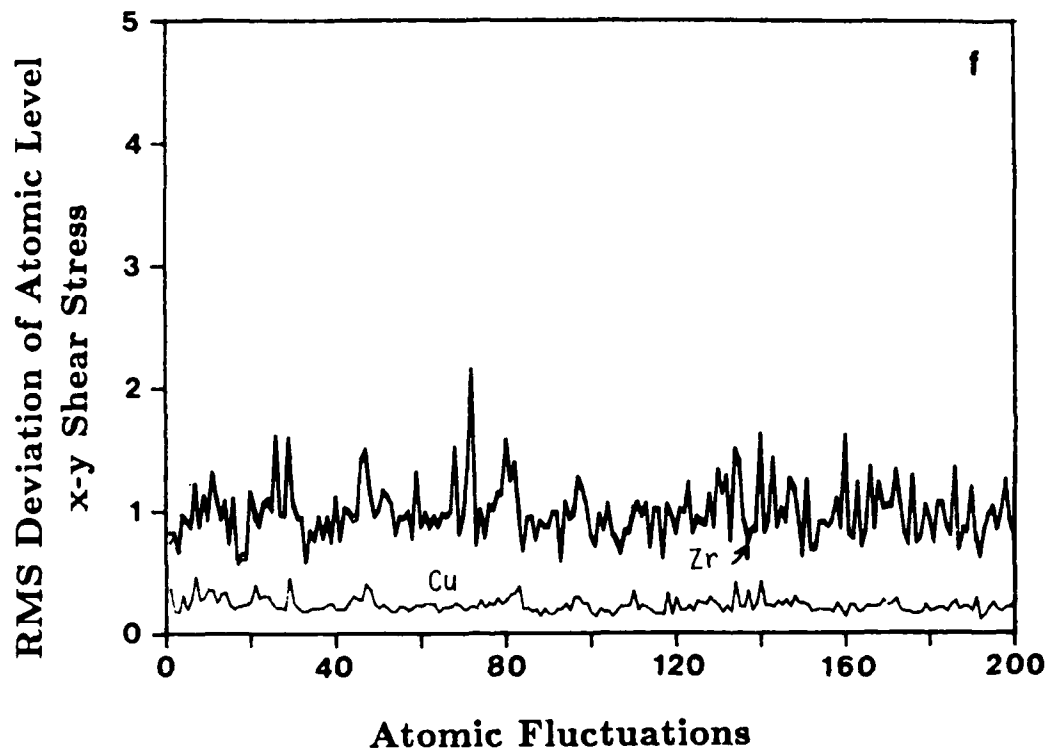


Fig. 2f

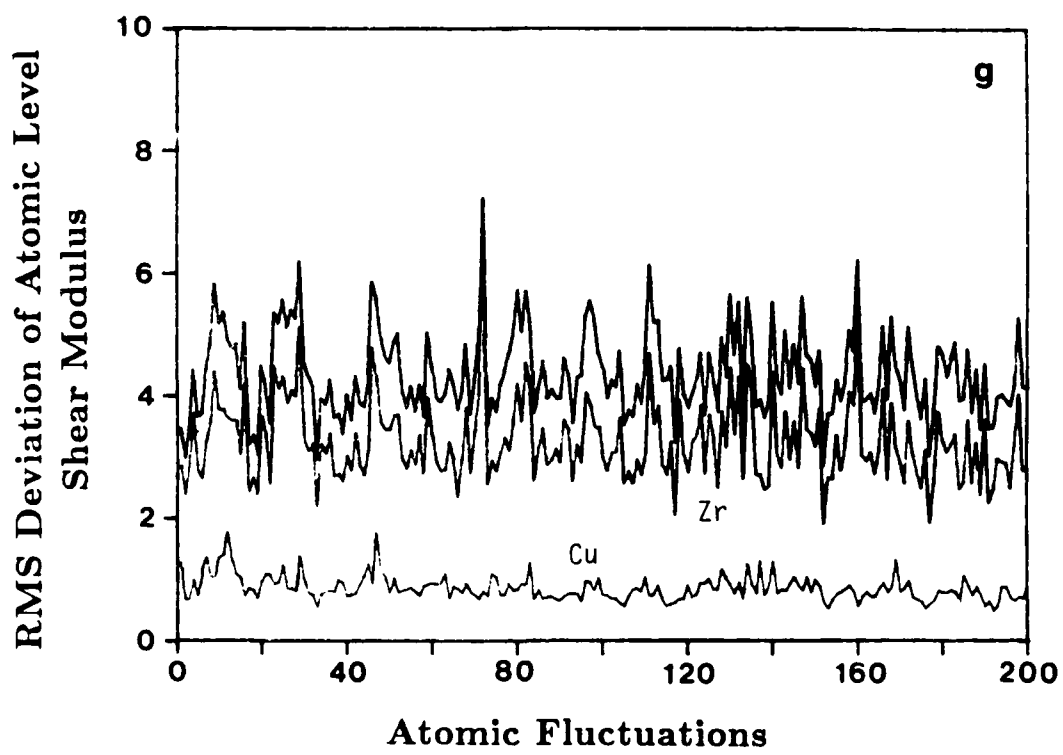
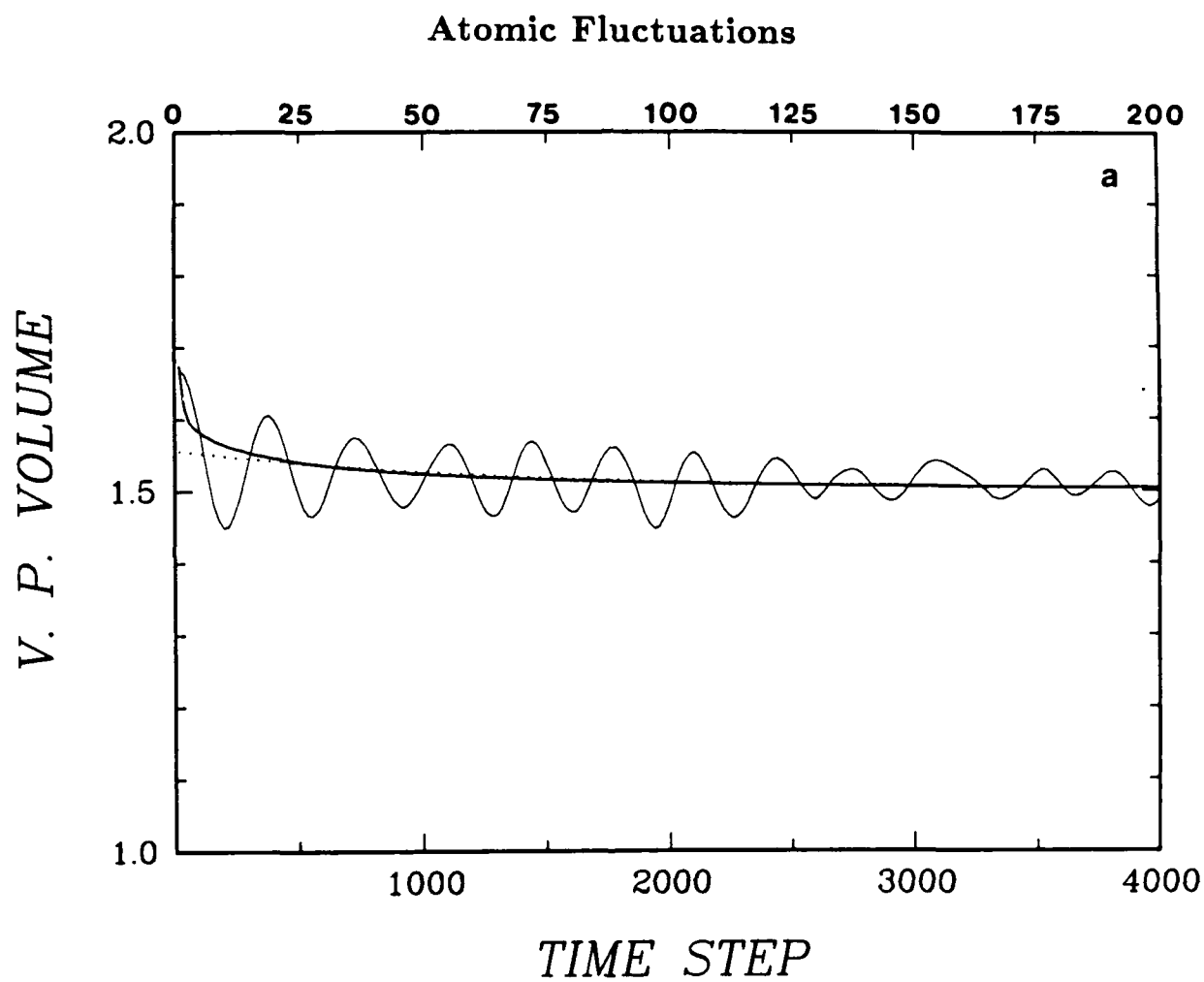


Fig. 2g



**Fig. 3** Best Williams-Watts function fits to the changes in ensemble averages for the same seven structure parameters given in Figs. 1 and 2.

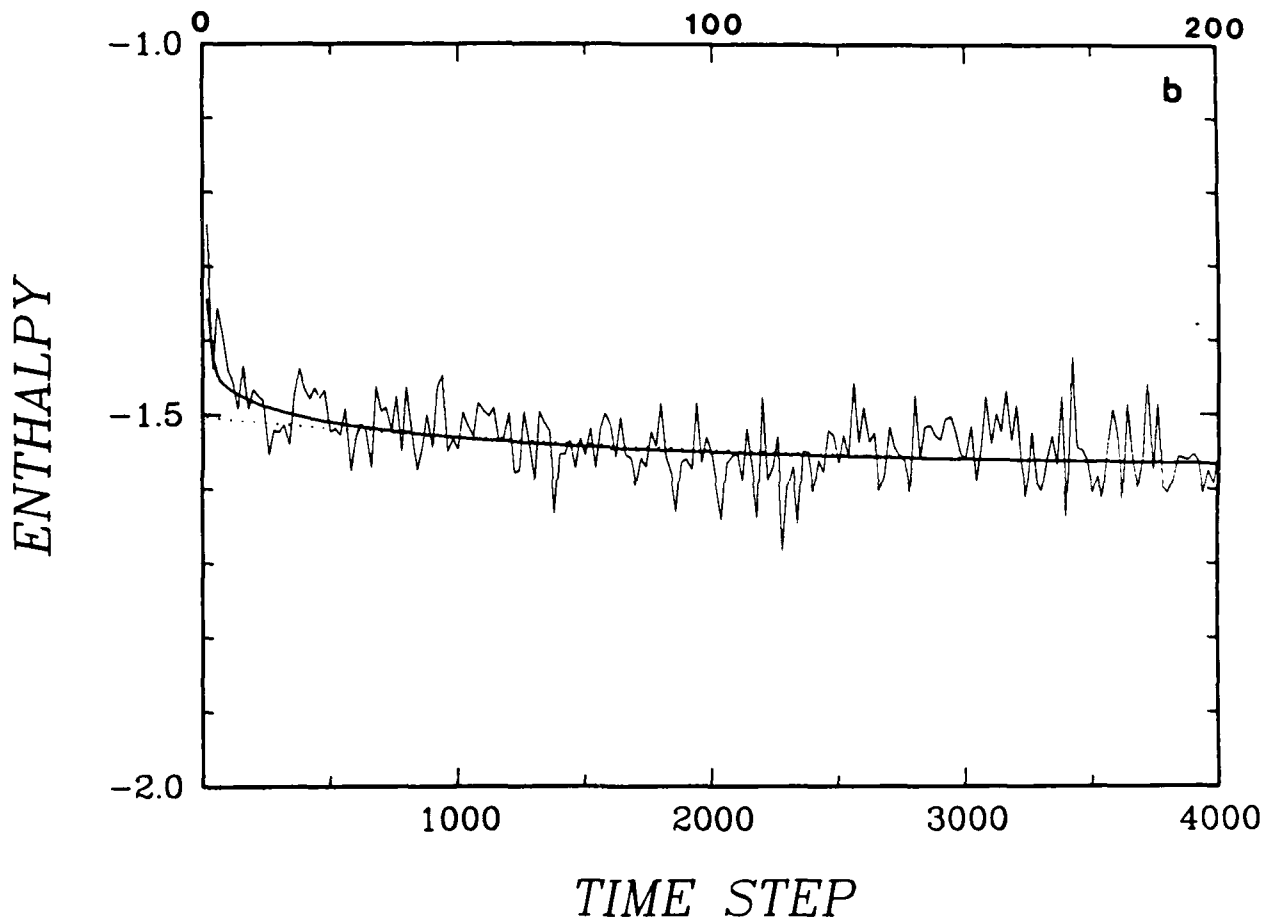


Fig. 3b

Atomic Fluctuations

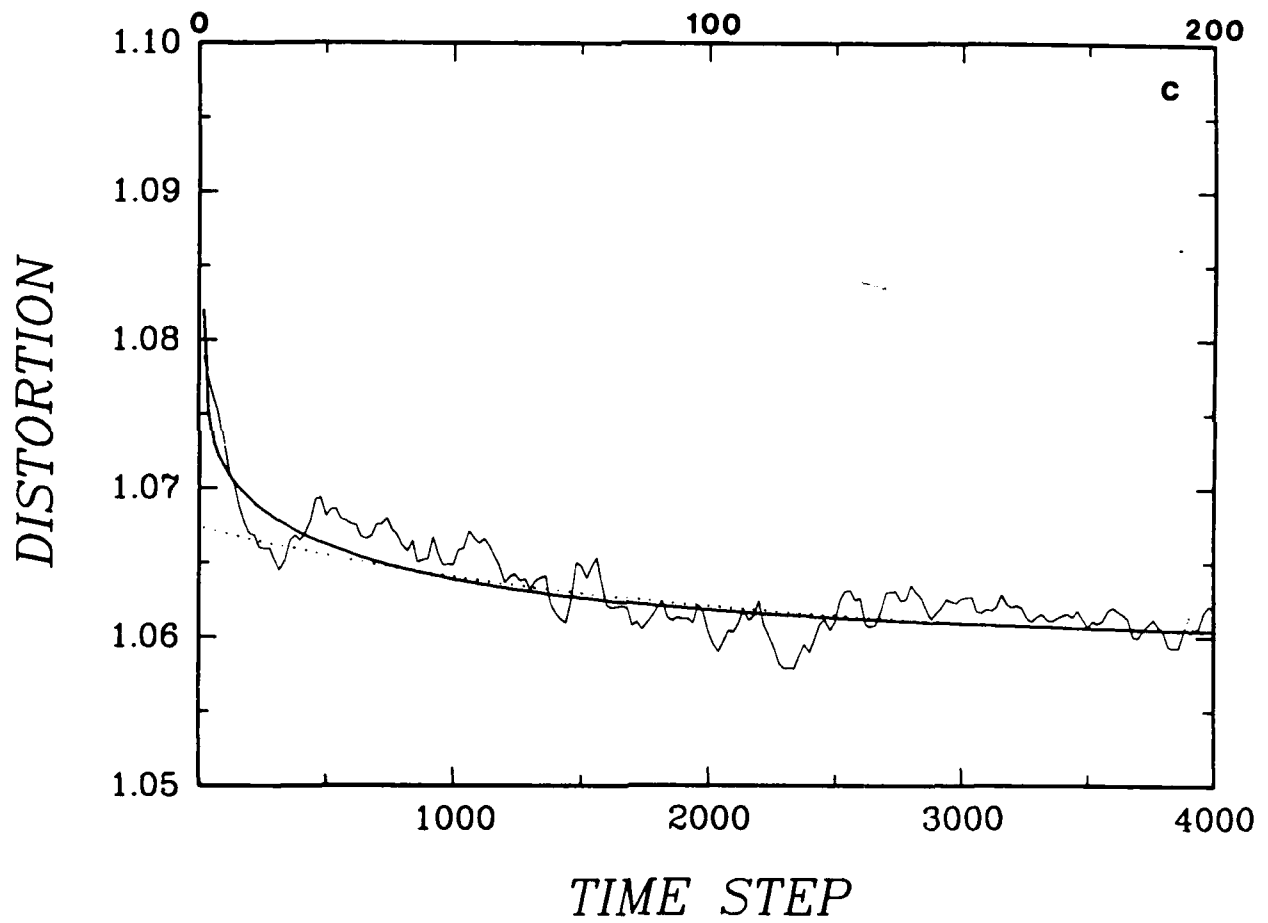


Fig. 3c

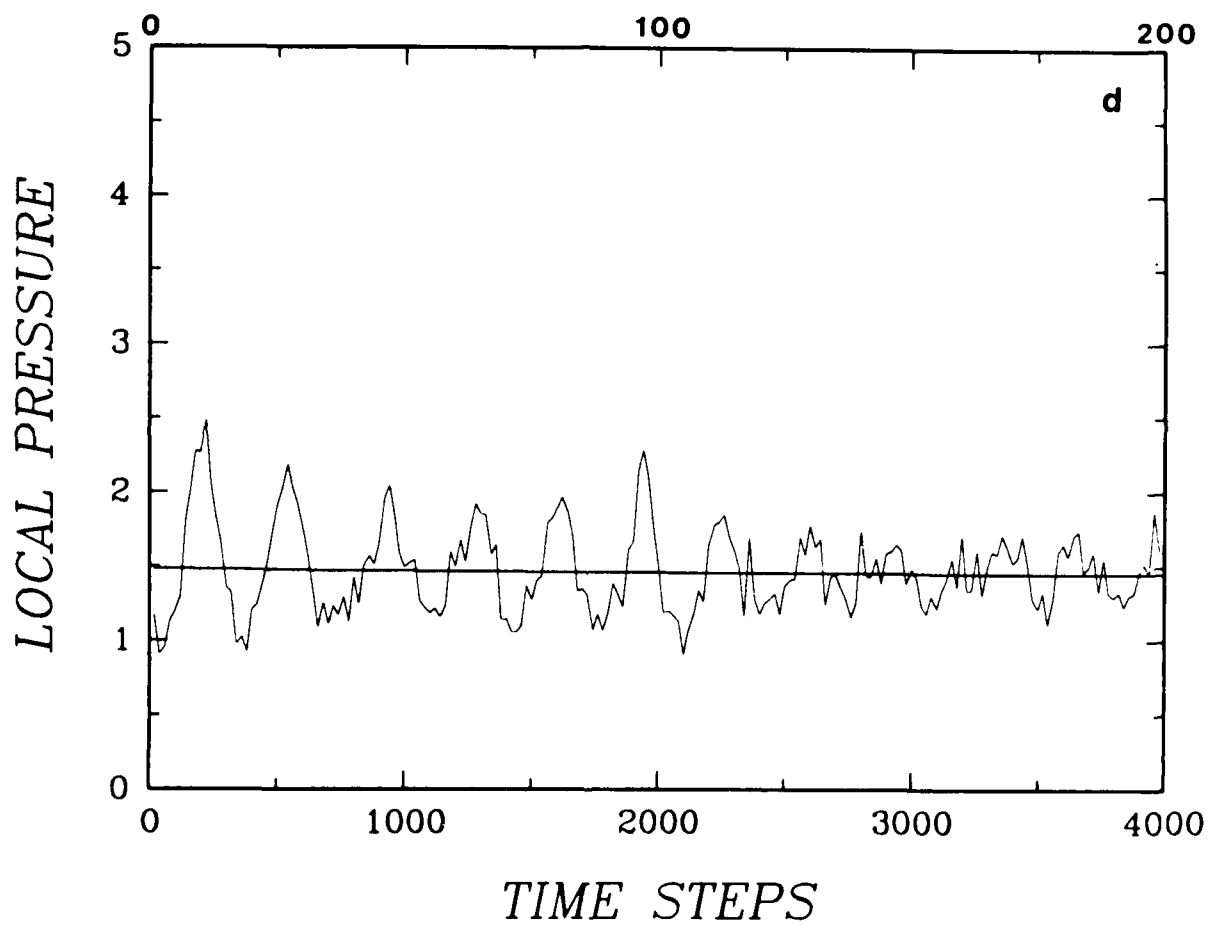


Fig. 3d

Atomic Fluctuations

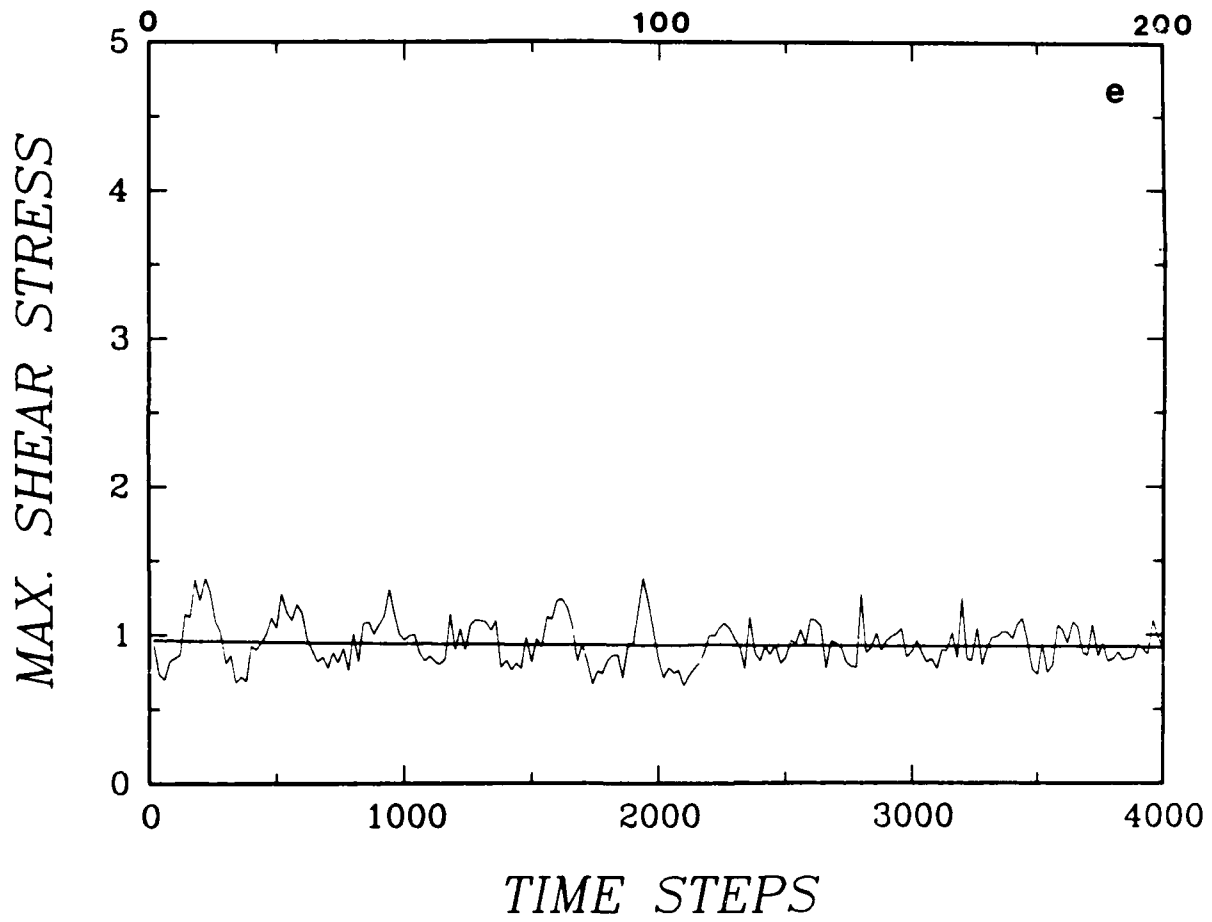


Fig. 3e

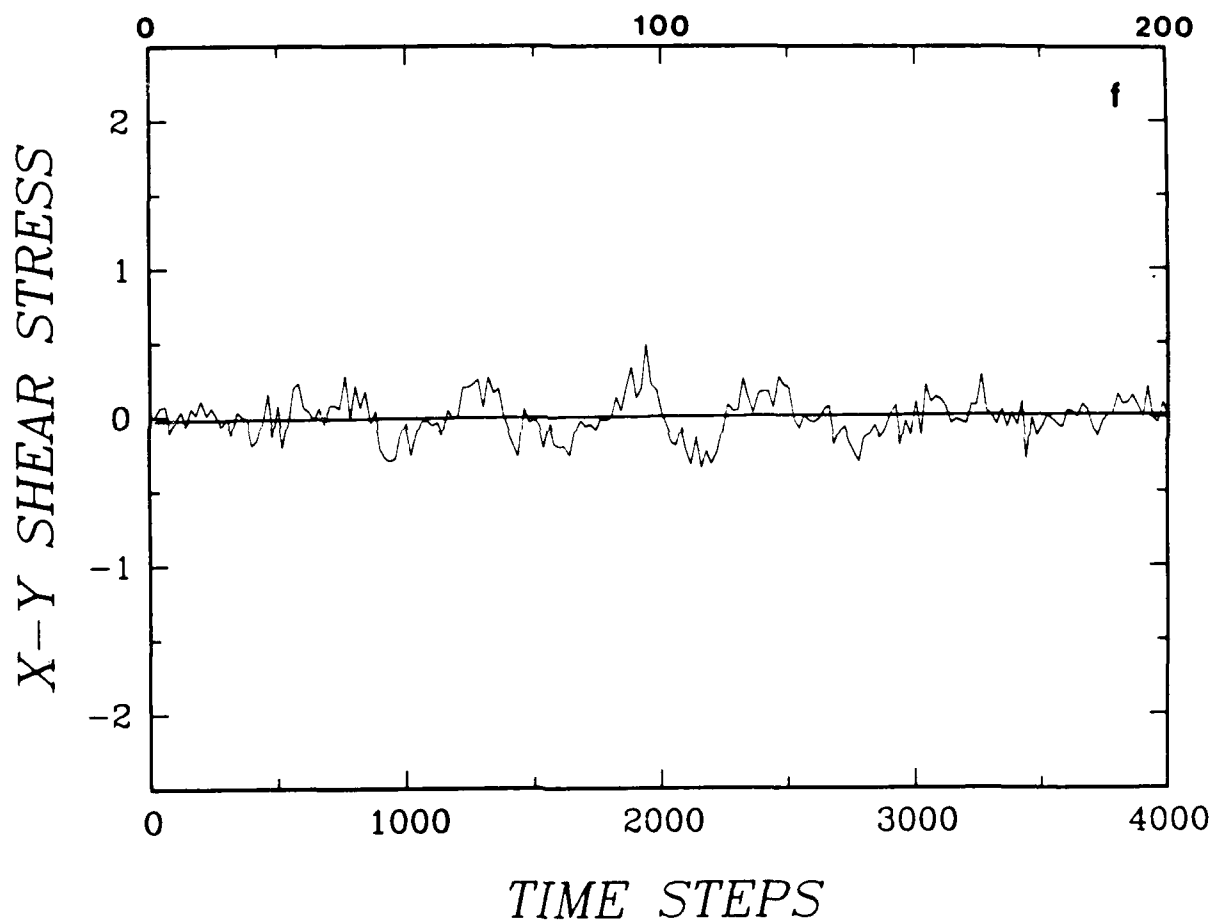


Fig. 3f

Atomic Fluctuations

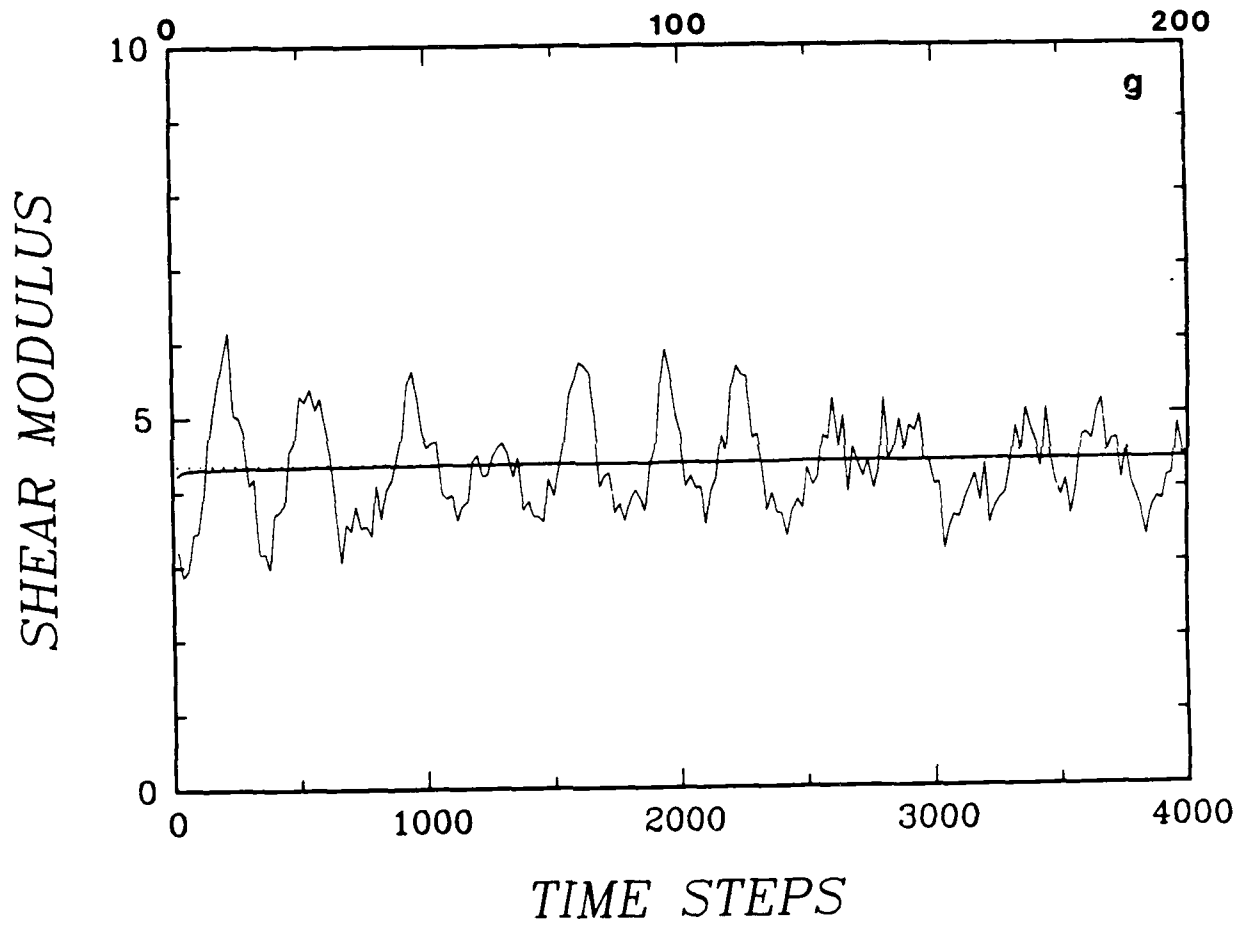


Fig. 3g

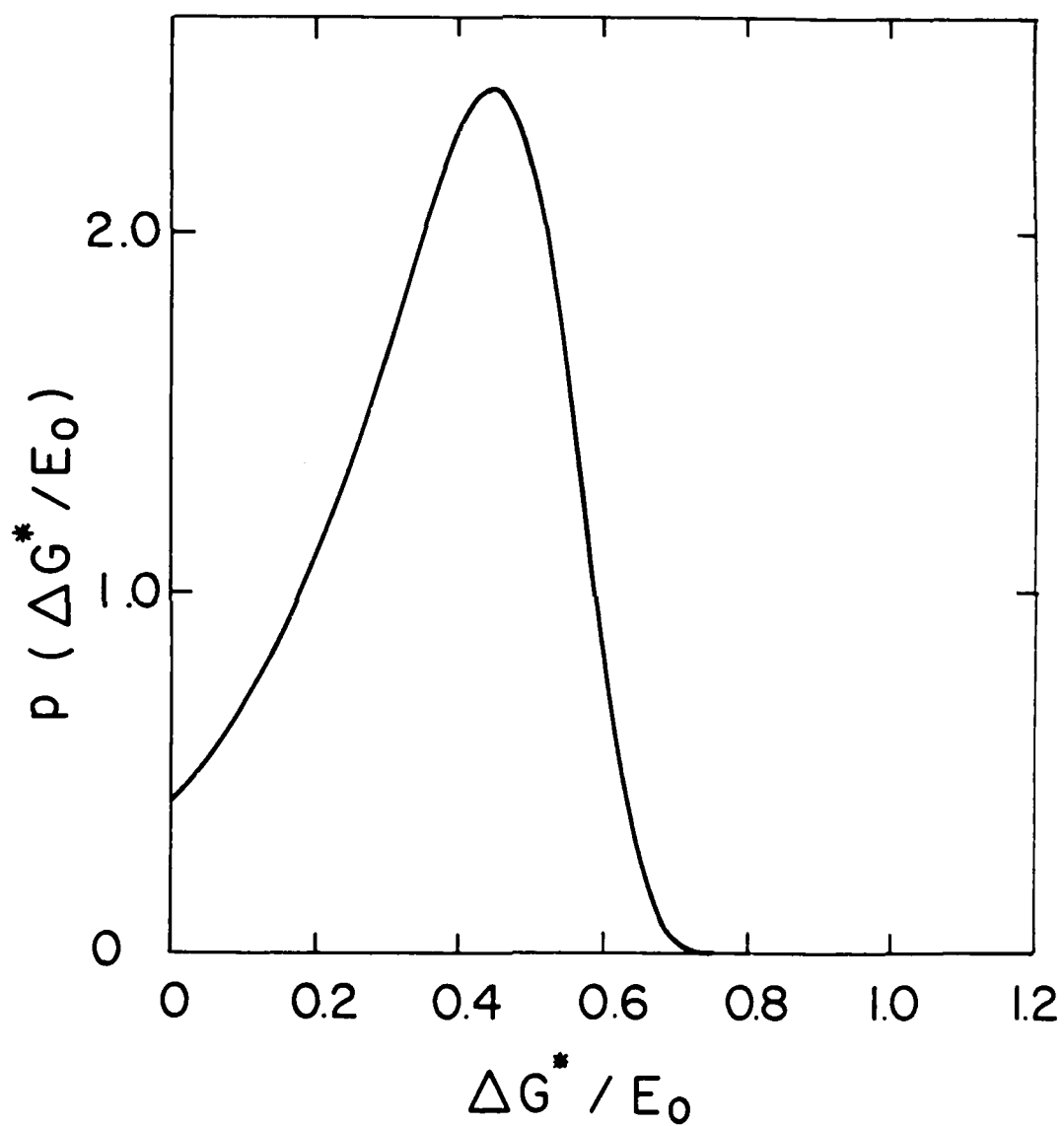


Fig. 4 The free energy barrier distribution function for the structural relaxations, obtained from the Williams-Watts distribution function by an operational inversion.

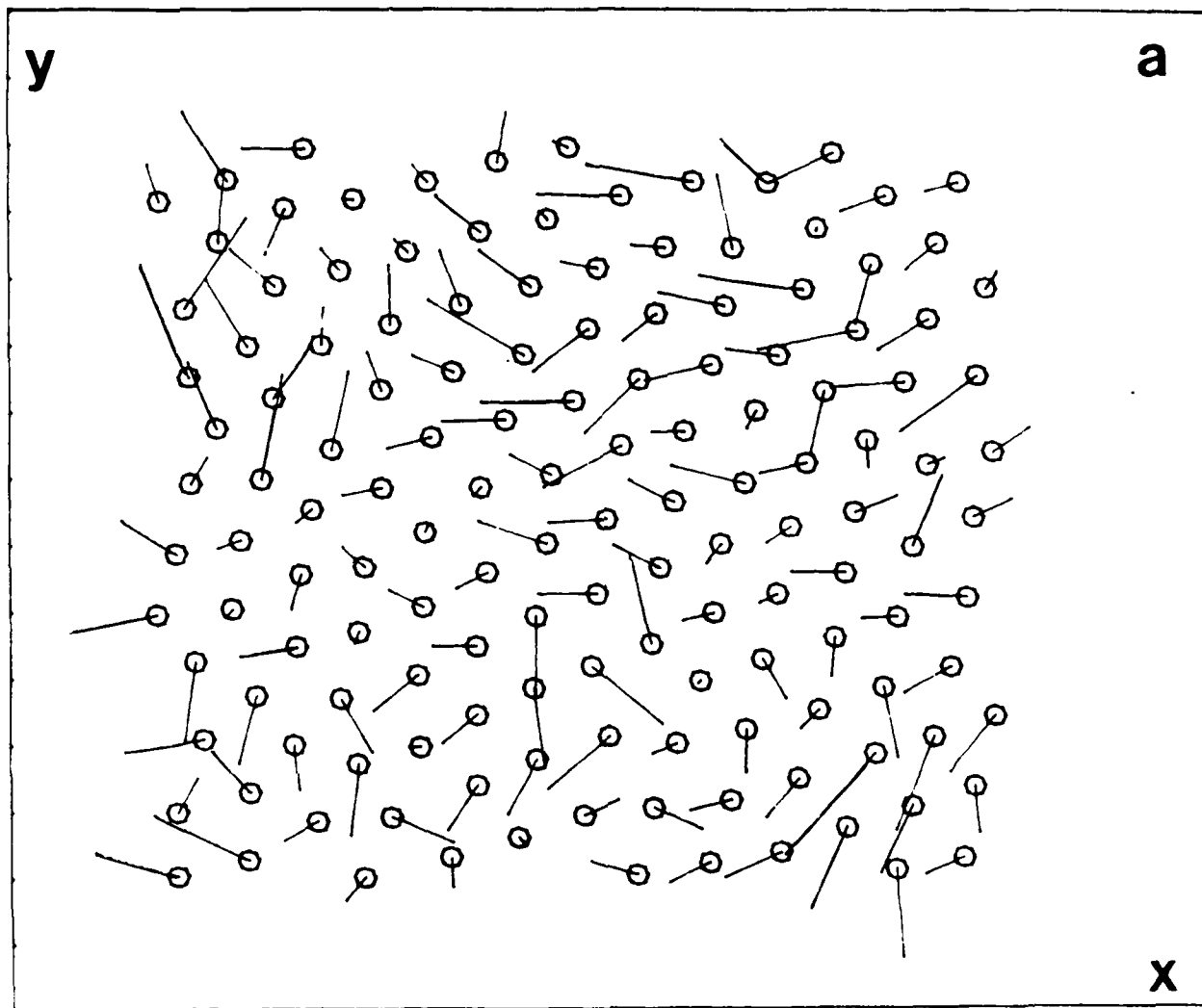


Fig. 5 Two different states of incremental atom displacements during the simulation: (a) for the period between 70-80 fluctuations, (b) for the period between 100-110 fluctuations.

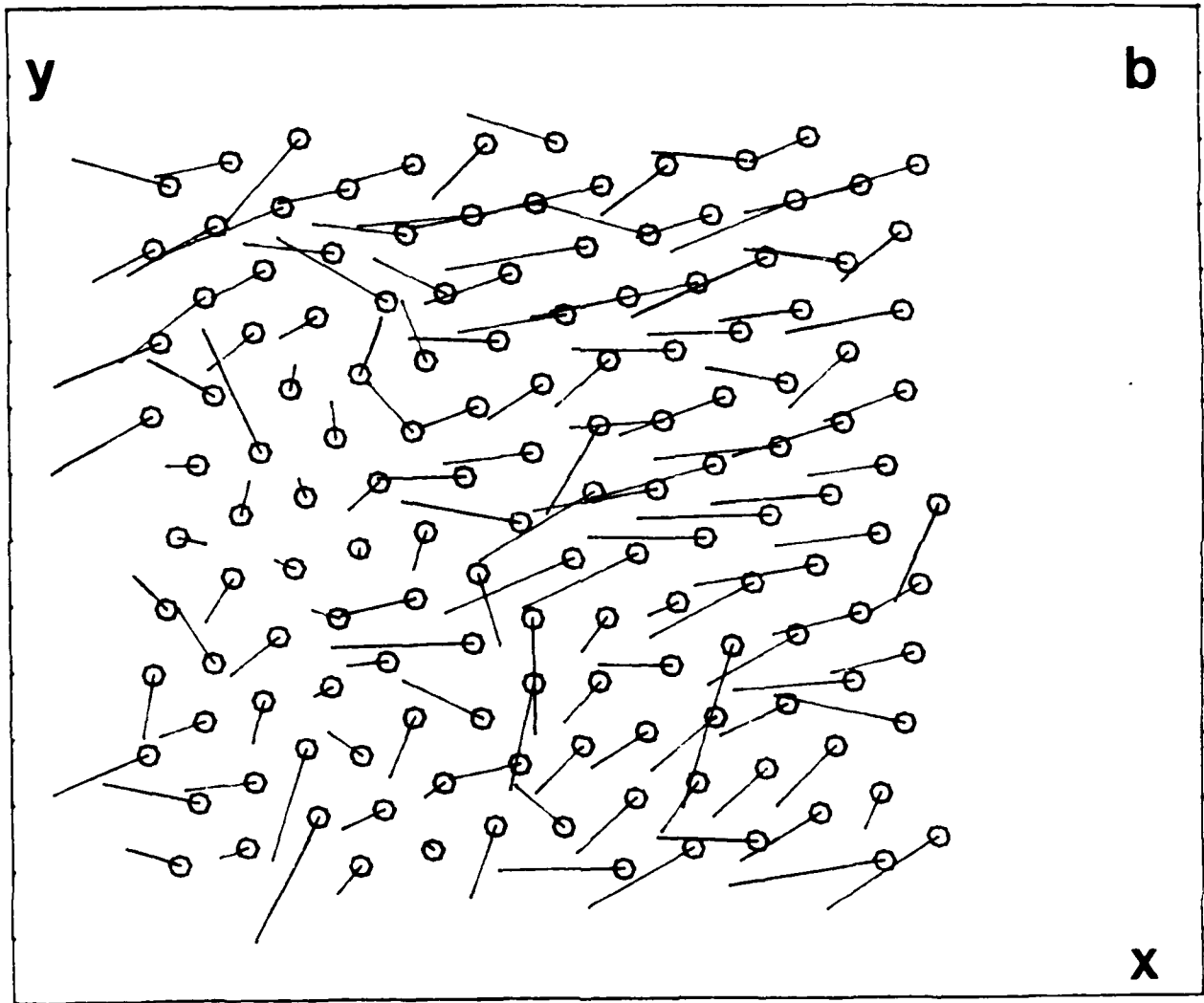


Fig. 5b

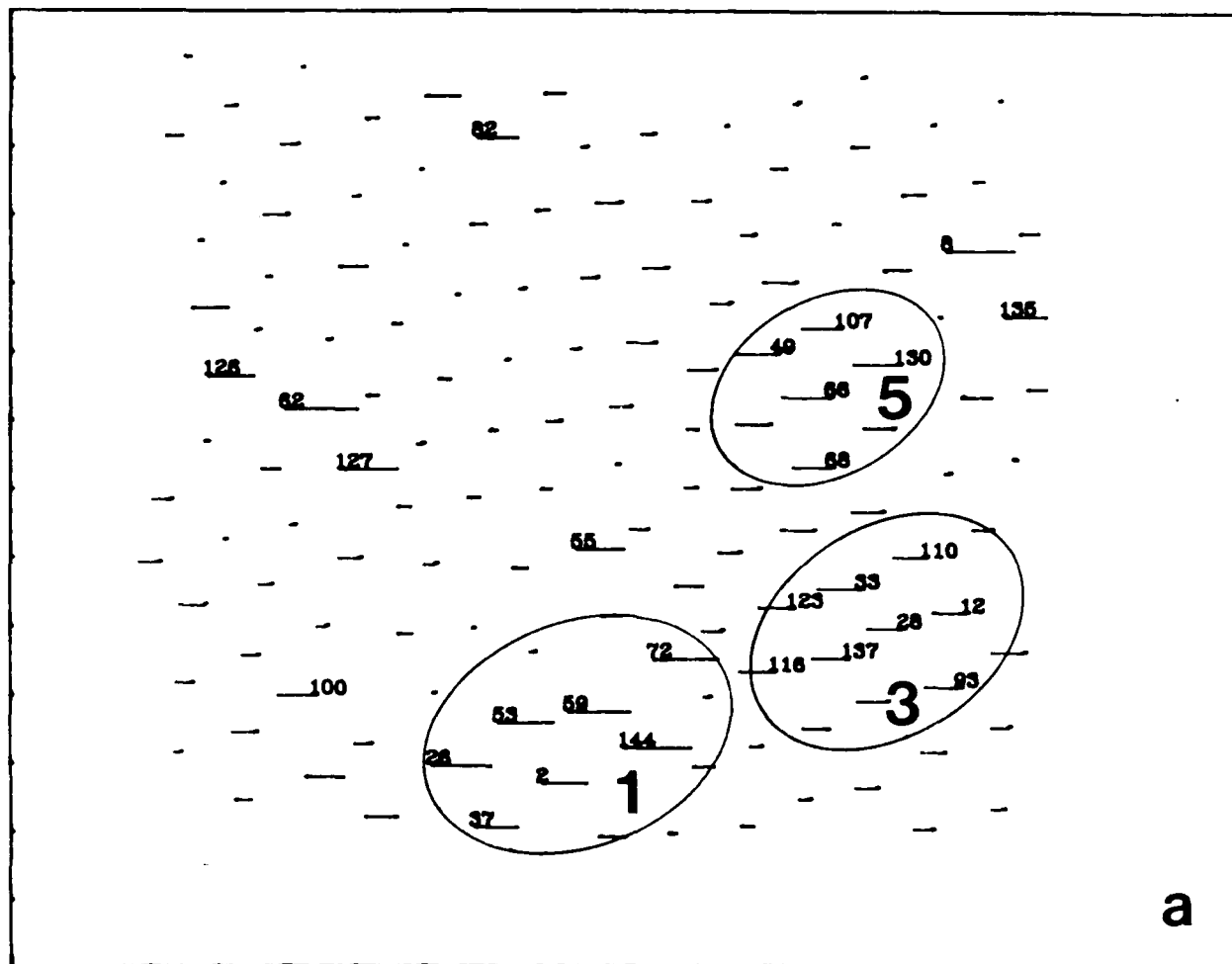


Fig. 6 Field of excess properties averaged over the entire simulation period:  
 (a) volume per atom, (b) enthalpy, (c) site distortion parameter.

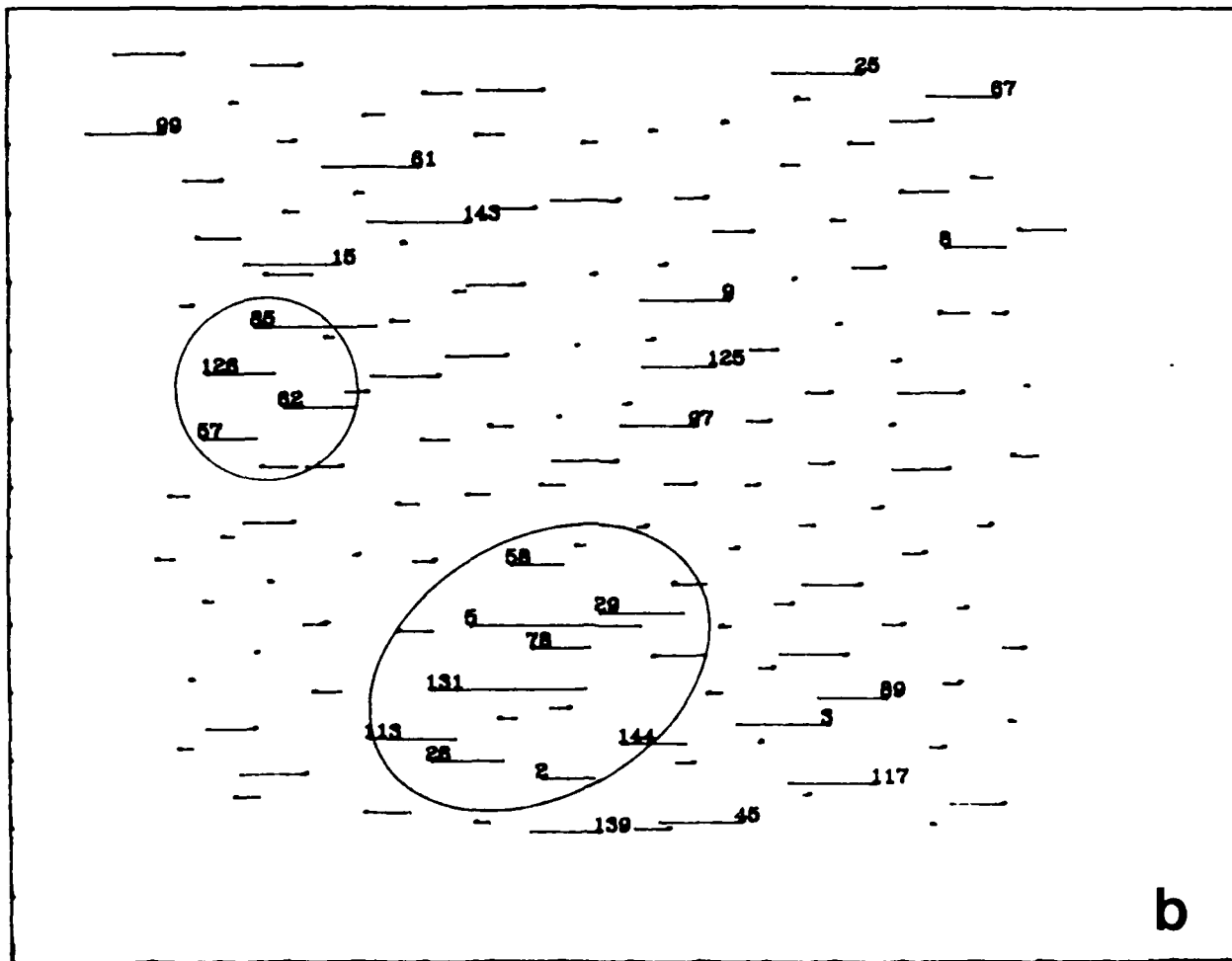


Fig. 6b

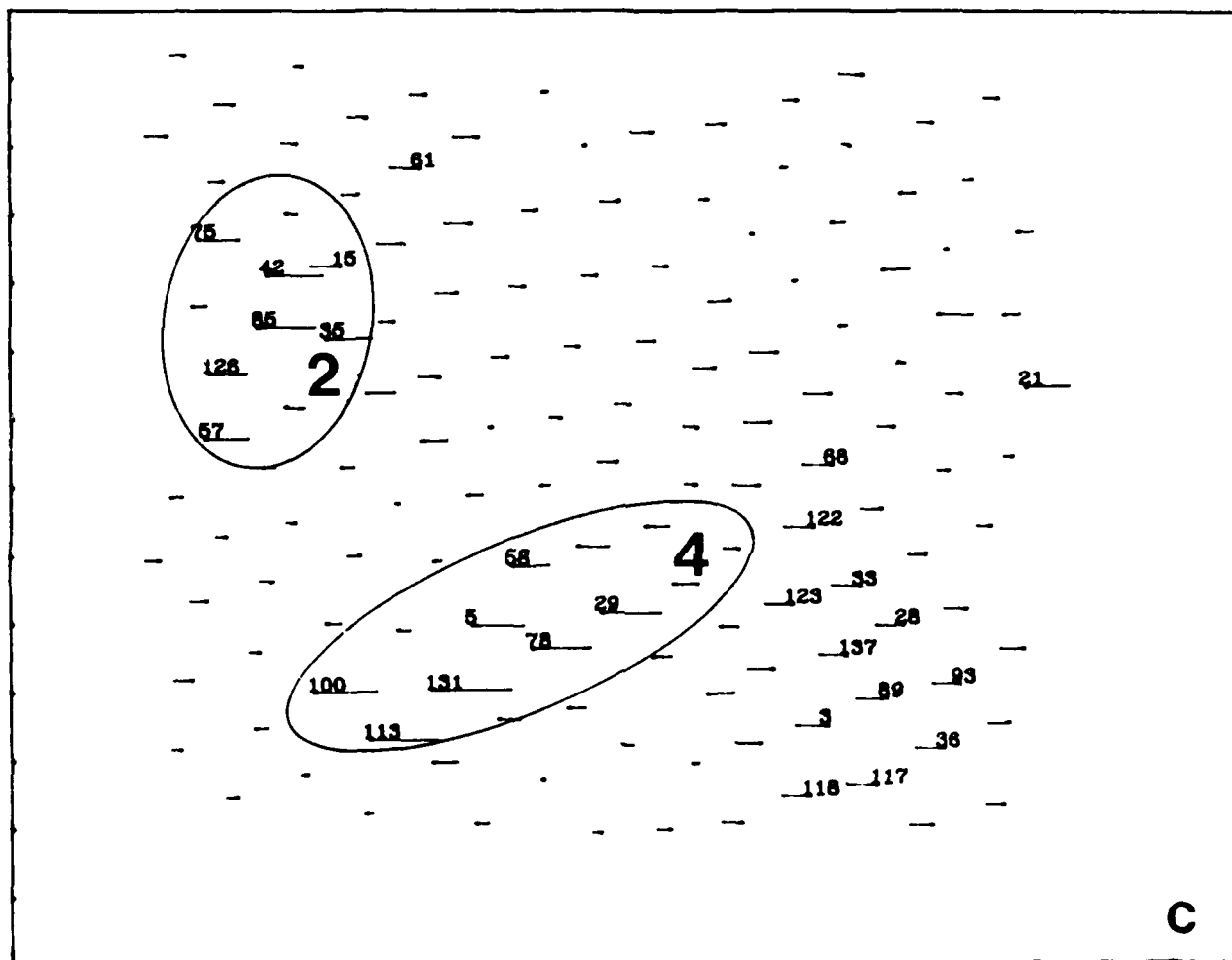


Fig. 6c

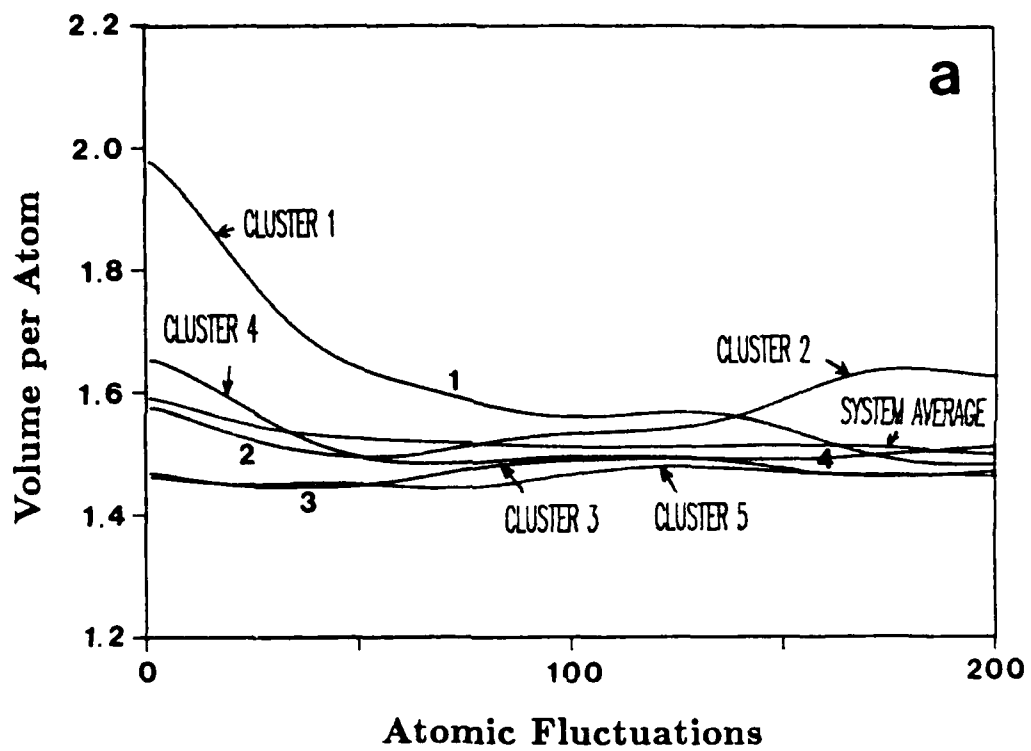


Fig. 7 Time dependent changes of the structure parameters in five selected clusters: (a) volume per atom, (b) enthalpy, (c) site distortion, (d) atomic site pressure, (e) atomic site maximum shear stress, (f) atomic site shear modulus.

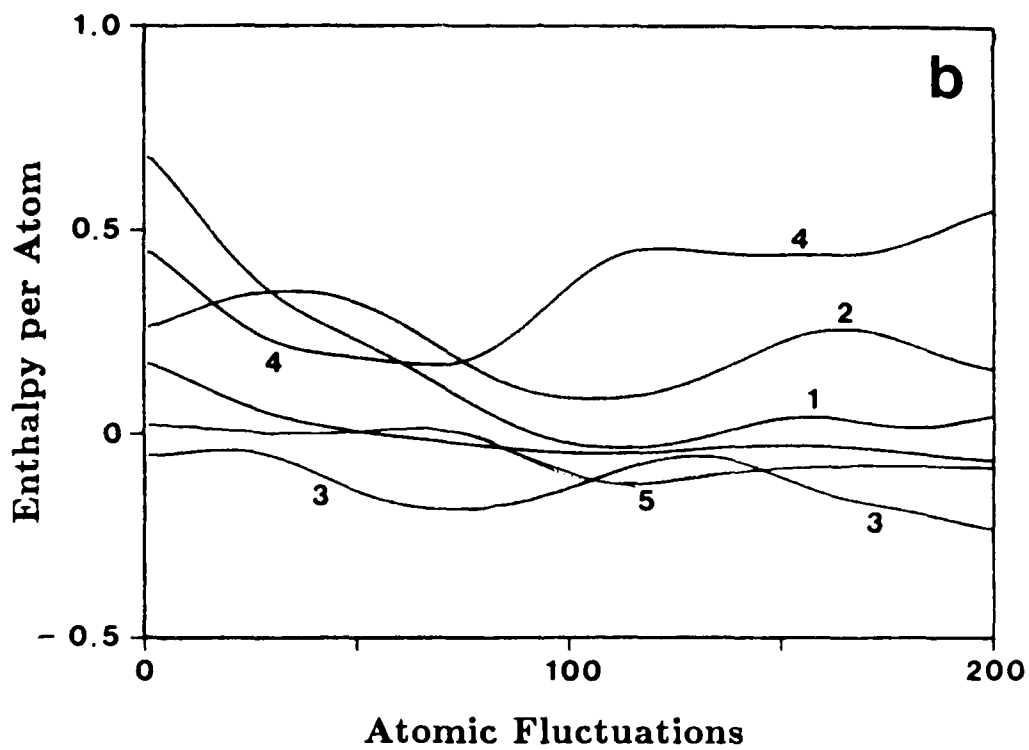


Fig. 7b

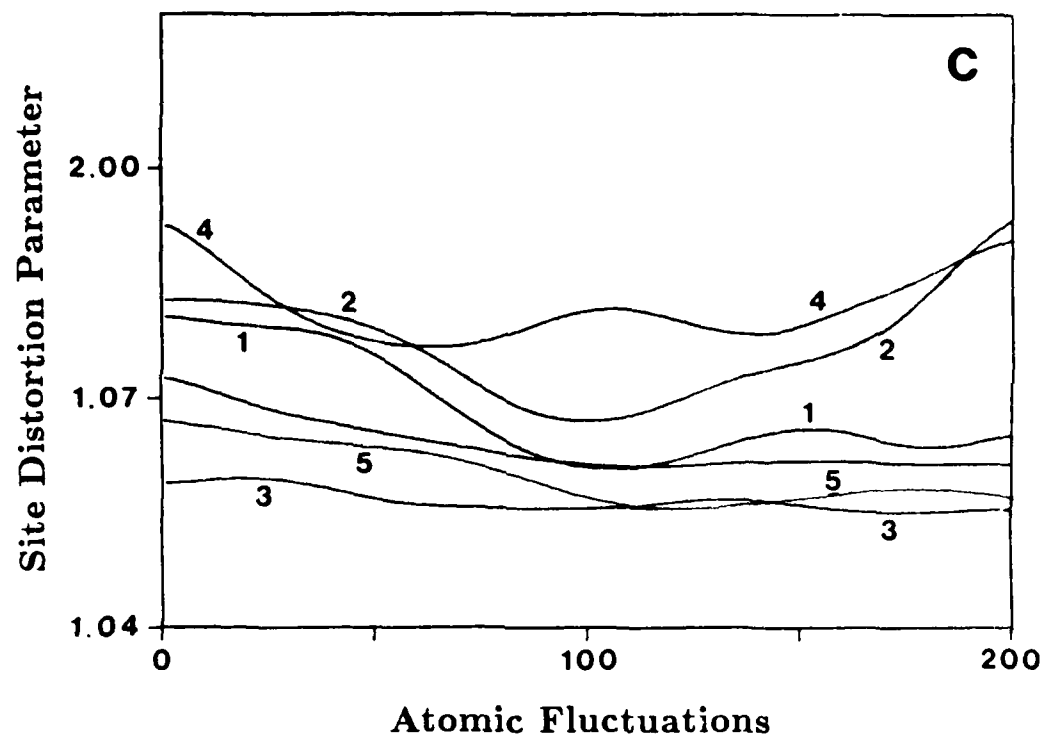


Fig. 7c

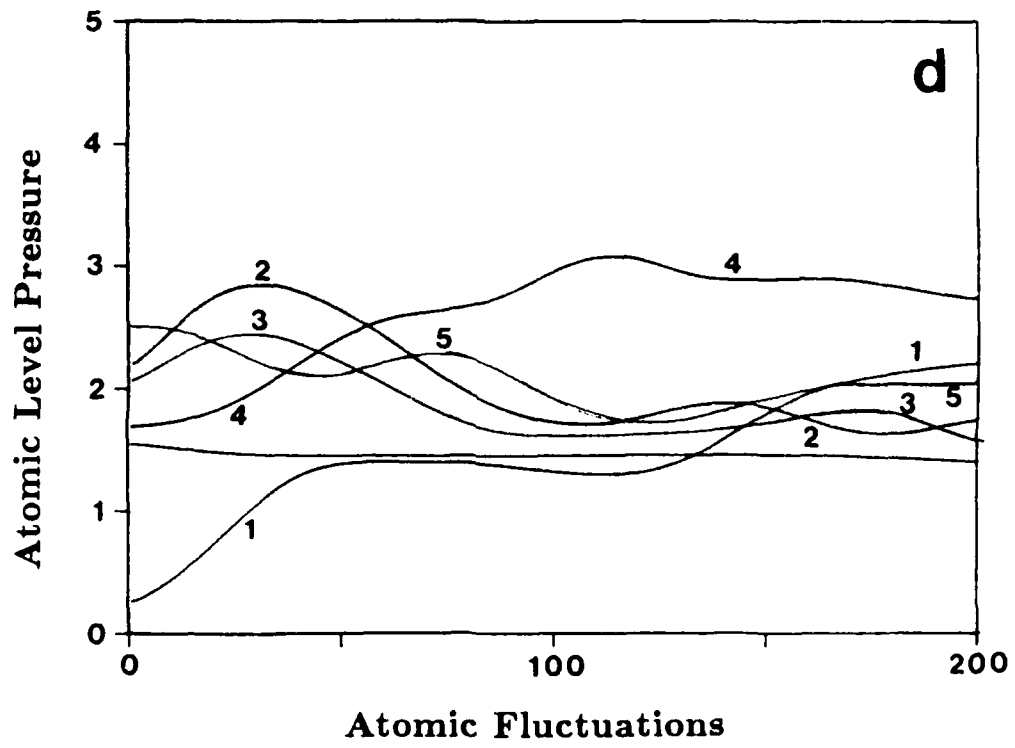


Fig. 7d

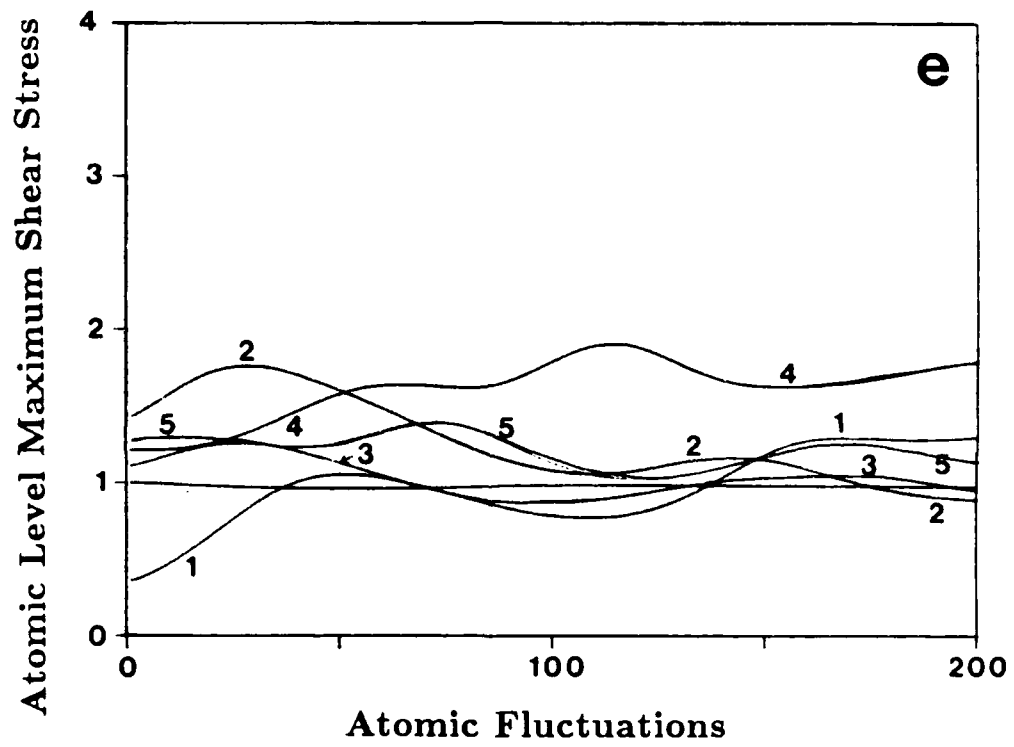


Fig. 7e

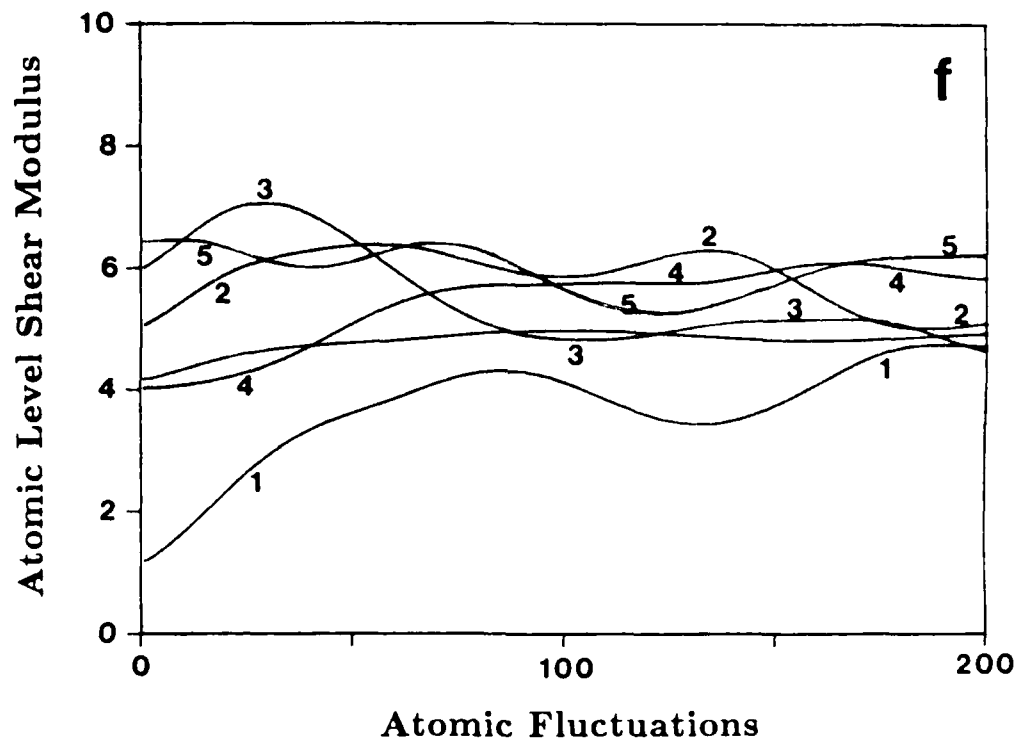


Fig. 7f

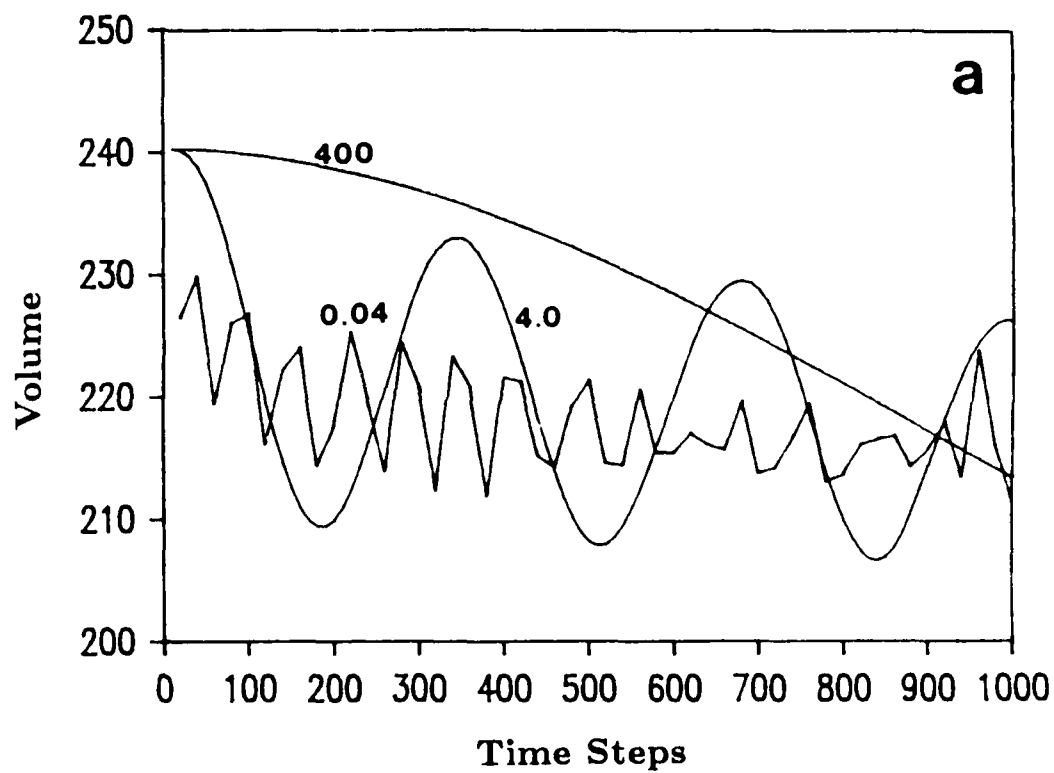


Fig. A1 Effect of choice of boundary mass on the relaxation of excess properties:  
 (a) volume per atom, (b) enthalpy, (c) atomic site pressure.

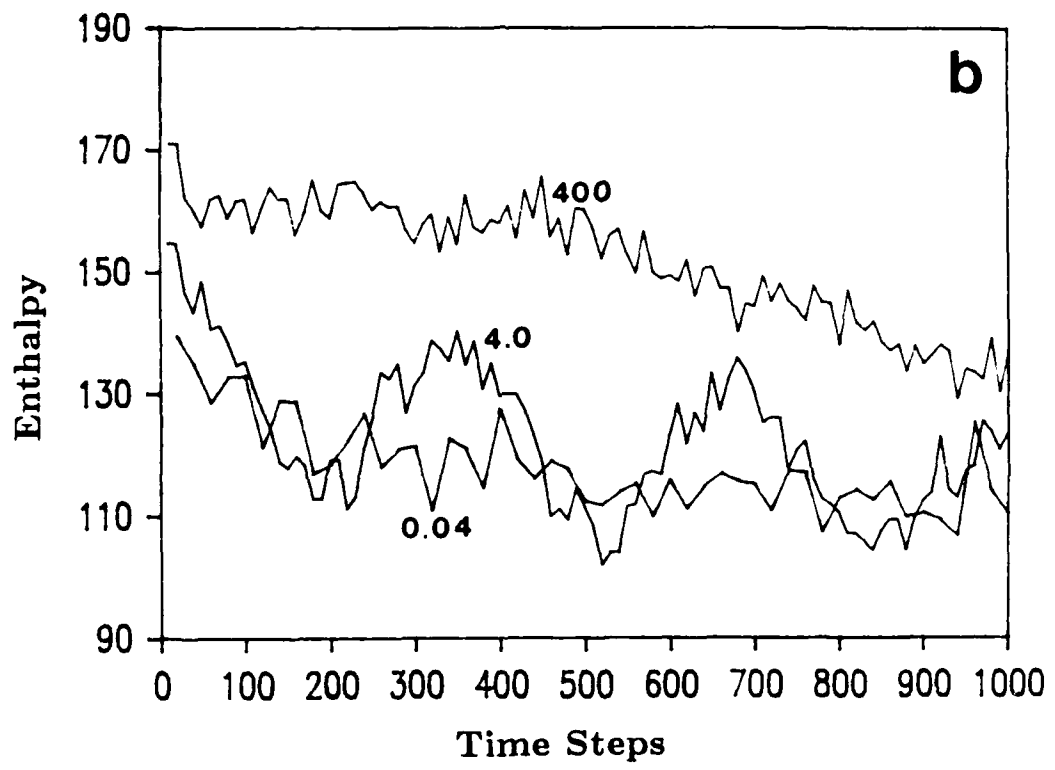


Fig. A1-b

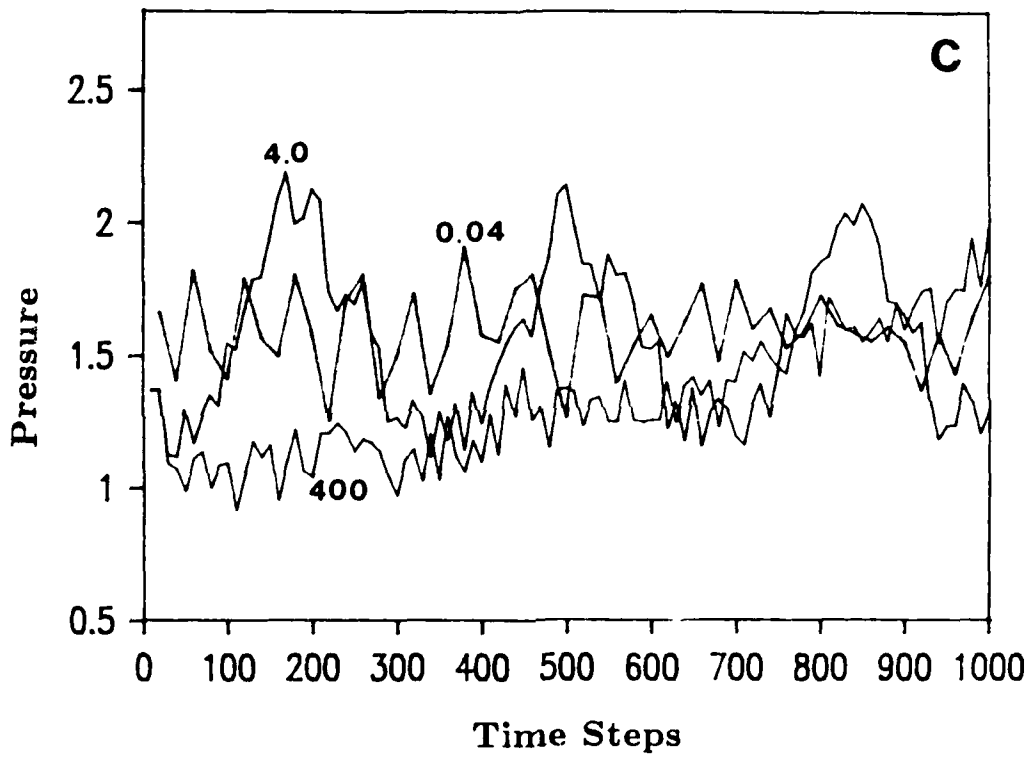


Fig. A1-c